A comparison of the DTRF2014, ITRF2014, and JTRF2014 solutions using DORIS

Guilhem Moreaux[1], Hugues Capdeville[1], Claudio Abbondanza[2], Mathis Bloßfeld[3], Jean-Michel Lemoine[4], and Pascale Ferrage[4]

[1] *Collecte Localisation Satellites, Ramonville Saint-Agne, France*

[2] *Jet Propulsion Laboratory – California Institute of Technology, Pasadena, USA*

[3] *Deutsches Geodätisches Forschungsinstitut at the Technische Universität München (DGFI-TUM), Munich, Germany*

[4] *Centre National d'Etudes Spatiales (CNES), Toulouse, France*

Abstract. In the context of the 2014 realization of the International Terrestrial Reference Frame (ITRF2014), the International DORIS Service (IDS) submitted to the International Earth Rotation and Reference Systems Service (IERS) a set of 1140 weekly solution files including station coordinates and Earth orientation parameters, covering the time period from 1993.0 to 2015.0. Then, in combination with the three other space geodetic contributions (GNSS, SLR and VLBI) to ITRF2014, the DGFI-TUM, the IGN, and the JPL IERS Combination Centres (CCs) computed their own TRF realizations denoted as DTRF2014 [Seitz *et al.*, 2016], ITRF2014 [Altamimi *et al.*, 2016], and JTRF2014 [Abbondanza *et al.*, 2017]. In this paper, we shortly present the computation procedures of the three TRF realizations to be able to interpret the obtained comparison results. However, the main objective of this study is to compare these three TRF realizations in terms of geocenter, scale, station positioning, and precise orbit determination (POD) performances based on the IDS contribution to ITRF2014 (IDS 09) and DORIS satellite localization from the IDS CNES-CLS analysis center. In case of the geocenter and scale realization, we found significant differences between the TRF solutions. The DTRF2014 shows the smallest total offset w.r.t. IDS 09 whereas the ITRF2014 shows the best overall performance. In terms of station position residuals, JTRF2014 performs best since this TRF includes non-linear station variations. For the DORIS POD, we found only differences at a very low level. As a summary, we can state that all TRF solutions agree very well with each other and that the obtained differences are very small. Nevertheless, the ITRF2014 solution shows the slightly best overall performance of all solutions.

Introduction

DORIS (Doppler Orbitography Radiopositioning Integrated by Satellite) is one of the four fundamental geodetic techniques contributing to the realization of the ITRS (International Terrestrial Reference System). Thus, early 2015, in the framework of the 2014 realization of the International Terrestrial Reference Frame (ITRF), the IDS [International DORIS Service; Willis *et al.*, 2010] delivered a set of 1140 files including weekly minimum constrained solutions of station coordinates and daily Earth orientation parameters, covering the time period from January 1993 to December 2015 [Moreaux *et al.*, 2016a] to the International Earth Rotation and Reference Systems Service (IERS). In addition to the DORIS data span, the IDS contributions to ITRF2008 and ITRF2014 differ by the number of multi-satellite weekly IDS analysis center solutions they are based on (7 for ITRF2008, 6 for ITRF2014), the DORIS observations (even over the common time period), and the DORIS measurement

modeling. Benefiting from the development of new models to correct the Jason-1 [Lemoine & Capdeville, 2006] and SPOT5 [Capdeville *et al.*, 2016] data for the South Atlantic Anomaly (SAA) effects, the new series includes Jason-1 data between the end of the TOPEX/Poseidon mission and the beginning of the Jason-2 mission and uses the SPOT5 SAA-corrected data starting on SPOT5 cycle 138 (2005/12/27). The IDS contribution to ITRF2014 also includes tracking data from the DORIS satellites launched after mid-2008: Jason-2, Cryosat-2, HY-2A and Saral. Note that all these new satellites carry on-board the latest generation of the DORIS receivers, the so-called DGXX receivers, which can track up to seven beacons simultaneously, resulting in a significant increase in the number of available measurements especially at lower elevations [Bloßfeld *et al.*, 2016b]. As a consequence of their low orbital altitudes (700–1340 km), the DORIS satellites are more sensitive to the time-variable geopotential [e.g. EIGEN-6S2, Rudenko *et al.*, 2014]. Then, the IDS analysis centers adopted geopotential models that included more detailed time-variable gravity modeling. Furthermore, the new IDS solution includes the implementation of beacon frequency offset estimations (i.e. difference between actual frequency and the nominal value) as well as DORIS ground antenna phase center variations [Tourain *et al.*, 2016]. As a result, compared to the IDS contribution to ITRF2008 [Altamimi *et al.*, 2011], the IDS contribution to ITRF2014 exhibits more accurate translation and scale parameters and vertical positioning performances are improved. For more details on the IDS contribution to ITRF2014, see Bloßfeld *et al.* [2016b]; Moreaux *et al.* [2016a]. From the IDS, the IGS (International GNSS Service), the ILRS (International Laser Ranging Service) and the IVS (International VLBI Service) submissions for the ITRF2014, the three IERS Combination Centres (CCs: DGFI-TUM, IGN and JPL) computed combined TRF solutions individually. The three CCs combine technique-specific products provided by the above mentioned services of the International Association of Geodesy (IAG). Thereby, the IGS and the IDS provide minimum constrained daily and weekly solutions whereas the ILRS provides loosely constrained weekly solutions. The only service which provides session-wise datum-free normal equations is the IVS. Since all of the four fundamental geodetic space techniques, namely GNSS, VLBI, SLR, and DORIS, have technique-specific strengths, highest accuracy of derived geodetic parameters can only be achieved in a rigorous combination of them as long as an appropriate weighting of the observations is adopted, local ties are provided and introduced, and velocity equality constraints are properly selected. Thus, to link the different techniques, one needs co-located sites: sites where two or more space geodesy instruments are operating and where the differential coordinates between the geodetic instruments are known (so called local ties). In addition to the availability of co-located sites, the TRF computation strongly depends on the segmentation of station

position time series into time intervals with constant velocity and without any coordinate jumps. While DGFI-TUM and IGN use the conventional least-squares approach to estimate mean positions and velocities at a reference epoch, JPL implemented the Kalman filtering approach [Wu *et al.*, 2015] to estimate weekly positions. Other examples of epoch-wise (sub-secular) estimated frames are given in Bloßfeld *et al.* [2014, 2016a]. In the JPL solution, the station position is modeled as a random walk driven by white noise whose variance is characterized by analyzing station displacements induced by temporal changes of planetary fluid masses (atmosphere, oceans and continental surface water). The main objective of this investigation is to show and analyze the impact of using one of the three ITRF2014 realizations while estimating precise positions of either DORIS stations or DORIS satellites. After a brief presentation of the three combination approaches and solutions, we evaluate geocenter and scale offsets between IDS 09 to the 3 TRF realizations. Then, we show the station position differences between the three 2014 TRF realizations and we evaluate these three solutions in terms of tie residuals w.r.t. surveyed ties. Afterwards, we analyze the impact of estimating the DORIS station positions from the three different TRF solutions on the precise orbit determination (POD) of three DORIS satellites: Topex/Poseidon, SPOT5 and Jason-2. Within the DORIS POD, the station coordinates are fixed to the different TRF realizations. A similar study for a POD of SLR satellites was done by Rudenko *et al.* [2017]. Moreover, for altimetry satellites, Zelensky *et al.* [2017] did some investigations. Finally, we provide recommendations in the use of the DTRF2014, ITRF2014, and JTRF2014 for those who are interested in the estimation of precise positions of either DORIS stations or DORIS satellites.

Characteristics of the DTRF2014, ITRF2014, and JTRF2014 solutions

This section briefly discusses the characteristics of each of the three evaluated ITRF realizations used in this paper. For further details, the reader is referred to Seitz *et al.* [2012] and Seitz *et al.* [2016] for the DGFI-TUM solution DTRF2014, to Altamimi *et al.* [2016] for the IGN solution ITRF2014, and to Abbondanza *et al.* [2017] for the JPL solution JTRF2014. The main characteristics are summarized in Table 1.

DTRF2014 from DGFI-TUM

The DTRF2014 solution was computed in a procedure originally developed for the computation of the DTRF2008 solution. A detailed description of the DGFI-TUM combination approach at the normal equation level of the least-squares adjustment process can be found in Seitz *et al.* [2012]. More details on the DORIS-specific solution of TRFs and EOPs which was incorporated into the DTRF2014 can be found at Bloßfeld *et al.* [2016b]. The IDS contribution to the DTRF2014 is a time series of weekly minimum constrained solutions with full

variance-covariance information reported in SINEX files. In a first step, datum-free normal equations (NEQs) are reconstructed by inverting the variance-covariance matrix and introducing similarity transformation parameters w.r.t. the origin, the orientation and the scale (7 parameter in total each week). The epoch-wise TRF solutions are screened for outliers and discontinuities which are introduced afterwards into the weekly NEQ system. In the so called intra-technique combination step, the datum-free NEQs are accumulated using equal weights each week. The parametrization of the epoch-wise available station coordinates is changed to one offset and one velocity estimated at a reference epoch. At the end of this step, the IDS contribution to the DTRF2014 comprise one multi-year NEQ containing station coordinates, velocities and epoch-wise given EOPs. The NEQs of the other geodetic space techniques are derived in a similar way with slight changes due to technique-specific aspects. In the inter-technique combination step, the technique-specific NEQs of the four geodetic space techniques DORIS, VLBI, SLR, and GNSS are combined. Equal parameters such as EOP at a common epoch are stacked. The relative weighting of the NEQs is based on the a posteriori variance factors of the single-technique solutions. The station coordinates and velocities are combined by introducing external constraints between the station coordinates (local ties) and between the velocities at one station (more than one technique operated at a station). The relative weighting of the local ties is done according to the residuals between the local tie and the 3D-difference between the technique-specific reference points in the single-technique solutions. The datum of the combined solution is realized as follows. The origin is implicitly realized within the SLR NEQ. This means, no translation constraints have to be introduced. The origin information is transferred via the local ties from the SLR station network to the other techniques. In a similar way, the scale of the combined NEQ is realized. The SLR- and VLBI-NEQ contain implicit information of the scale. Before combination, the SLR- and VLBI-only scales are compared. Since DGFI-TUM founds that they are equal, it is valid to treat the scales as one common scale in the combination which means that this information is transferred via the local ties to the DORIS and GNSS station network. The orientation is realized by a no-net-rotation (NNR) condition applied to a selected subnet of GNSS stations (stable time series and long observation time span). Again, this information is distributed to the other technique-specific networks via the local ties. From the datum realization described above it is obvious that the quality of the estimated solution strongly depends on the quality and the global distribution of the introduced local ties. Therefore, it is often stated in the literature that currently, the main limiting factor of the global TRF accuracy are the local ties.

ITRF2014 from IGN

Globally, the IGN procedure to compute the ITRF2014 [Altamimi *et al.*, 2016] is very similar to the one used for the previous ITRF realizations such as ITRF2005 [Altamimi *et al.*, 2007] and ITRF2008 [Altamimi *et al.*, 2011]. Therefore, the ITRF2014 realization can be seen as a two step process: 1) stacking of individual time series to get a long-term solution per technique including station positions and velocities at a reference epoch as well as daily EOPs; and 2) combining the four space geodesy technique long-term solutions with local ties at the co-located sites. Similar to the past ITRF solutions, the ITRF2014 long-term (mean) origin coincides with the Earth system center of mass as observed by the SLR technique over the full ITRF2014 time span (i.e. 1993.0–2015.0) whereas the ITRF2014 scale is defined as the weighted mean of the SLR and VLBI intrinsic scales. Moreover, IGN still makes use of velocity constraints to force nearby stations or multiple segments of the same station to have the same velocity. The station position time series discontinuities were identified by the visual inspection of the time series. In addition, to ensure the consistency between all the techniques, while an earthquake happened at one site, the same discontinuity epoch was used for all the techniques present at that site. However, this new IGN solution differs to the previous ITRF realizations by the addition in the time series analysis of both annual and semi-annual signals as well as post-seismic deformation (PSD) for sites affected by major earthquakes. The modelization of the periodic signals is limited to the sites with sufficient time-span (longer than 2 years) and is realized by the addition to the stacking of sinusoidal functions. While the estimation of the periodic seasonal signals is done per technique, the PSD parameters are fitted to the GNSS station position time series only. In overall, 13 DORIS stations from 7 sites are associated to PSD corrections. Due to the lack of a co-located GNSS receiver at the epoch of the earthquake, some DORIS sites (ex: Cibinong – Indonesia, Colombo – Philippines) which faced some Earthquakes do not take benefit of a logarithmic and/or exponential motion modeling. If the motion of a station was modeled with a PSD correction then, not computing the corrections to be added to the linear model would introduce position errors at the decimeter level. As the periodic signals are deduced from the coordinate time series, they must contain not only geophysical phenomena (such as atmospheric and hydrological non-tidal one) but also technique systematic errors. Altamimi *et al.* [2016] reported that estimating the annual and semi-annual signals allows to reduce the velocity formal errors by about 10 %.

JTRF2014 from JPL

The Kalman filter and smoother for reference frame combination (KALREF) developed at the Jet Propulsion Laboratory combines observations of station positions as determined from VLBI, SLR, GNSS

and DORIS and EOP measurements along with the data measurement covariance matrices. Local tie observations at ITRF co-located sites are also assimilated during the combination and adopted as constraints to tie the technique-specific TRF. KALREF allows TRFs to be realized at a sub-secular time scale. The filter assimilates observations at a fixed weekly time step and includes options for constraining the station positions to move linearly or to move linearly and seasonally. Through the use of stochastic models for the process noise of the state vector parameters consisting of station positions, velocities, EOPs and the frame defining parameters (the Helmert transformation parameters), the station positions can be constrained to follow the linear or linear plus seasonal models (by setting the process noise variance to zero), to recover temporally unconstrained state parameters close to the observed station positions (by setting the process noise variance to a large value) or to follow a smoothed path (by setting the process noise variance to an intermediate value).

JTRF2014, in particular, adopts a dynamical model describing the evolution of the station positions based upon trend, annual, and semi-annual oscillatory modes. Unlike ITRF and DTRF realizations, JTRF makes use of position process noise to describe the non-secular and non-seasonal component of the Earth deformation. White-noise driven random walk is chosen to represent the station position process noise. Site-dependent variances were determined by analyzing the non-seasonal and non-secular component of the Earth elastic response to terrestrial fluid redistributions. EOPs and Helmert transformation parameters instantly mapping the combined frame to the space-geodetic inputs are also modeled as random walk driven by white noise, with variances sufficiently large to accommodate the week-to-week fluctuations of the Earth rotation and the Helmert parameters variations.

JTRF2014 frame definition is accomplished by setting to zero the SLR translational parameters and by sequentially estimating translational parameters from GNSS, DORIS and VLBI to SLR during the measurement update. This entails the SLR origin is not being adjusted during the assimilation. Likewise, scale Helmert parameters of VLBI and SLR are set to zero whereas the scale of GNSS and DORIS inputs is being adjusted to the weighted (through the inverse of the covariance matrices of the observations) average of VLBI and SLR scale. As a result of that, JTRF2014 provides a sub-secular (weekly) frame whose origin is the quasi-instantaneous CM (as detected by SLR) and whose scale is the quasi-instantaneous scale from VLBI and SLR.

Tie vectors are applied at the epoch of their measurement and each of the tie constraints is weighted through the inverse of the measured covariance matrices scaled by properly selected variance factors. The optimal set of tie variance factors has been empirically determined as

Table 1: *Main features of the DTRF2014, ITRF2014 and JTRF2014 DORIS solutions.*

Solution	DTRF2014	ITRF2014	JTRF2014
Producer	DGFI-TUM	IGN	JPL
Post-seismic deformation	No	Yes	No
Technique-specific velocity constraints	No	Yes	Yes
Nb of files	1	1	1838
Nb of sites	71	71	71
Nb of stations	153	160	159
Nb of discontinuities	56	62	13
Nb of velocities	148	127	-
Nb of vertical velocities with $\sigma \leq 1$ mm/yr	123	196	-
Nb of horizonal velocities with $\sigma \leq 1$ mm/yr	106	160	-

a function of the agreement between space-geodetic and terrestrial observations.

Co-motion constraints have also been applied during the JTRF2014 assimilations. Such constraints dictate the equivalence of the displacements observed by nearby stations at co-located sites and they require (i) the trend variable (i.e. the velocity) of co-located stations be equivalent, (ii) the seasonal oscillator parameters relevant to co-located instruments be the same, (iii) the station position process noise of co-located stations be characterised by a 1.0 correlation coefficient.

Table 2: *Main statistics of the transformation parameters of the IDS 09 series wrt DTRF2014, DTRF2014ntc, ITRF2014, ITRF2014asc and JTRF2014. Units are mm and mm/yr.*

Time	Datum	Scale			T_x			T_y			T_z		
span		mean	trend	std	mean	trend	std	mean	trend	std	mean	trend	std
	DTRF2014	1.51	0.59	4.00	2.35	-1.33	5.76	5.73	-1.78	5.76	1.45	1.92	20.64
	DTRF2014ntc	1.99	0.58	4.01	2.64	-1.37	5.89	5.71	-1.76	5.71	2.77	1.80	20.41
1993.0	ITRF2014	7.52	0.25	3.94	-1.28	-0.08	5.75	-2.47	-0.59	5.85	-3.83	3.26	20.70
2002.4	ITRF2014asc	7.56	0.25	3.87	-1.30	-0.08	5.20	-2.57	-0.59	5.28	-3.84	3.29	20.49
	JTRF2014	16.19	-1.38	4.23	-0.31	-0.54	5.94	2.36	-1.86	5.99	-3.26	3.80	20.32
	DTRF2014	5.37	-0.20	2.11	-0.98	-0.02	3.85	-0.33	-0.27	4.00	-18.59	-3.05	12.11
	DTRF2014ntc	5.22	-0.19	2.16	-1.10	0.06	4.07	-0.54	-0.24	3.56	-19.14	-3.12	12.01
2002.4	ITRF2014	8.78	-0.15	2.06	-1.01	0.01	3.90	1.50	0.06	3.99	-17.68	-2.93	12.11
2008.5	ITRF2014asc	8.80	-0.14	1.97	-0.94	0.07	3.03	1.48	-0.06	3.38	-17.68	-2.94	12.04
	JTRF2014	10.36	-0.09	2.30	-1.36	-0.08	3.99	-0.13	0.25	3.52	-17.41	-3.30	12.33
	DTRF2014	2.86	1.13	2.04	-0.43	0.93	3.32	-1.48	0.34	3.71	-7.76	1.72	9.39
	DTRF2014ntc	2.79	1.07	1.91	-0.60	0.90	3.48	-1.29	0.28	3.07	-8.14	1.50	9.51
2008.5	ITRF2014	7.62	1.48	2.15	-2.50	0.33	3.40	-0.70	-0.23	3.67	-8.40	1.04	9.37
2015.0	ITRF2014asc	7.64	1.49	2.04	-2.53	0.38	3.36	-0.55	-0.25	2.83	-8.37	1.01	9.43
	JTRF2014	7.59	1.11	2.07	-2.96	0.02	3.44	-4.85	-0.87	2.94	-8.74	0.65	9.64

Table 3: *Station position WRMS of IDS 09 w.r.t. DTRF2014, DTRF2014ntc, ITRF2014, ITRF2014asc, and JTRF2014. Unit is mm.*

Time span	Datum	East		North		Up	
		mean	std	mean	std	mean	std
1993.0-2002.4	DTRF2014	16.97	2.24	12.13	2.04	14.79	2.15
	DTRF2014ntc	16.97	2.24	12.11	2.04	14.81	2.15
	ITRF2014	17.10	2.21	12.29	2.05	14.95	2.16
	ITRF2014asc	17.04	2.21	12.12	2.03	14.72	2.13
	JTRF2014	16.60	2.18	11.34	1.93	13.60	2.04
2002.4-2008.5	DTRF2014	10.26	1.85	7.53	1.26	8.61	1.59
	DTRF2014ntc	10.34	1.84	7.54	1.24	8.62	1.58
	ITRF2014	10.68	1.89	7.86	1.32	9.05	1.61
	ITRF2014asc	10.44	1.87	7.60	1.34	8.75	1.63
	JTRF2014	10.30	1.82	7.15	1.20	8.09	1.54
2008.5-2015.0	DTRF2014	8.03	1.17	6.36	1.10	7.25	1.10
	DTRF2014ntc	8.05	1.17	6.32	1.10	7.14	1.08
	ITRF2014	8.37	1.15	6.61	1.06	7.60	1.15
	ITRF2014asc	8.27	1.11	6.26	1.00	7.14	1.06
	JTRF2014	7.97	1.11	5.90	1.06	6.59	1.00

Comparisons between DTRF2014, ITRF2014 and JTRF2014

From the previous sections on the presentation of the three solutions, we first note that while DGFI-TUM and IGN estimate mean positions and velocities at a mean reference epoch by the least-squares technique (see Fig. 1 and 2), JPL combines the four space geodetic time series using a Kalman filter to produce weekly positions. Furthermore, the three IERS CCs differ in the handling of constraints in their inversion processes. For example, DGFI-TUM handles velocity equality constraints to force the same value over multiple segments unless a velocity discontinuity was observed (e.g. due to an earthquake) very carefully. Therefore, in the DTRF2014 solution, at any station and any time span corresponds one velocity vector while, in the ITRF2014 solution, for one station several time intervals can rigorously have an identical velocity. That explains why the DTRF2014 solution comprises more velocity vectors than the ITRF2014 (see Fig. 1 and 2) and presents larger formal errors for their velocities (which might be more realistic). For each DORIS station and each time period from the DTRF2014 solution, we identified the corresponding ITRF2014 velocity and computed both the horizontal and vertical velocity differences as depicted in Fig. 3. For the sites with ITRF2014 post-seismic corrections, the time periods corresponding to the post-seismic corrections were removed as they do not correspond

Table 4: *Amplitude of annual, semi-annual, 118-120, and 58-59 days signal in geocenter of IDS 09 wrt DTRF2014, DTRF2014ntc, ITRF2014, ITRF2014asc and JTRF2014. Unit is mm.*

Time	Datum	T_x				T_y				T_z			
span		365	183	118	59	365	183	118	59	365	183	118	59
	DTRF2014	2.98	1.15	-	1.36	3.59	-	-	-	-	-	5.16	-
	DTRF2014ntc	-	1.28	-	1.39	3.54	-	-	-	-	-	5.21	-
1993.0	ITRF2014	-	1.24	-	1.33	3.58	-	-	-	-	-	5.15	-
2002.4	ITRF2014asc	-	1.19	-	1.17	1.44	-	-	-	-	-	5.19	-
	JTRF2014	3.69	0.96	-	1.35	3.62	-	-	-	-	-	5.18	-
	DTRF2014	3.22	0.97	0.83	-	3.44	1.20	-	-	-	-	3.62	3.17
	DTRF2014ntc	3.39	-	-	-	2.10	1.31	-	-	-	-	3.63	3.05
2002.4	ITRF2014	3.11	0.96	0.79	-	3.35	1.28	-	-	-	-	3.49	3.13
2008.5	ITRF2014asc	-	-	0.84	-	-	-	-	-	-	-	3.56	3.10
	JTRF2014	3.45	-	-	-	1.97	1.39	-	-	-	-	3.56	3.14
	DTRF2014	1.59	1.27	2.50	0.86	3.53	-	1.31	1.67	-	-	5.65	-
	DTRF2014ntc	2.02	1.28	-	0.85	2.02	-	1.37	1.65	-	-	5.56	-
2008.5	ITRF2014	-	1.30	2.49	-	3.43	-	1.29	1.60	-	-	5.65	-
2015.0	ITRF2014asc	-	1.03	2.54	0.82	0.97	-	1.38	1.59	-	-	5.72	-
	JTRF2014	2.22	0.63	2.49	0.85	1.69	-	1.35	1.61	-	2.09	5.79	-

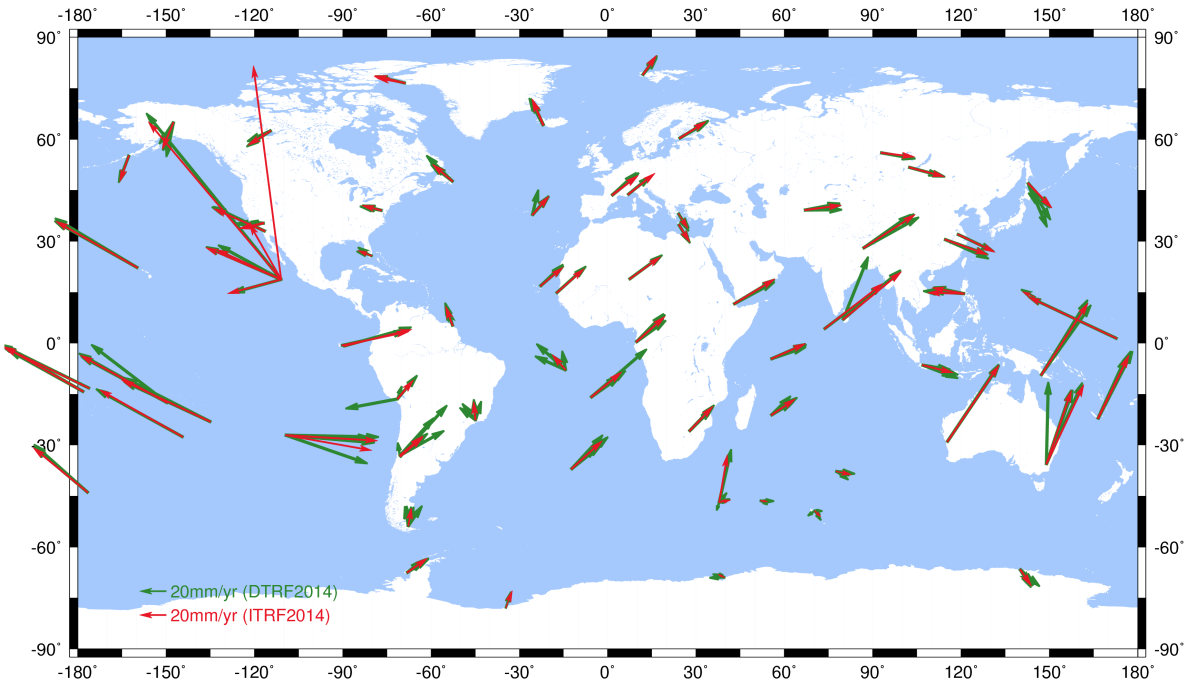

Fig. 1: *Horizontal DORIS velocities from DTRF2014 and ITRF2014.*

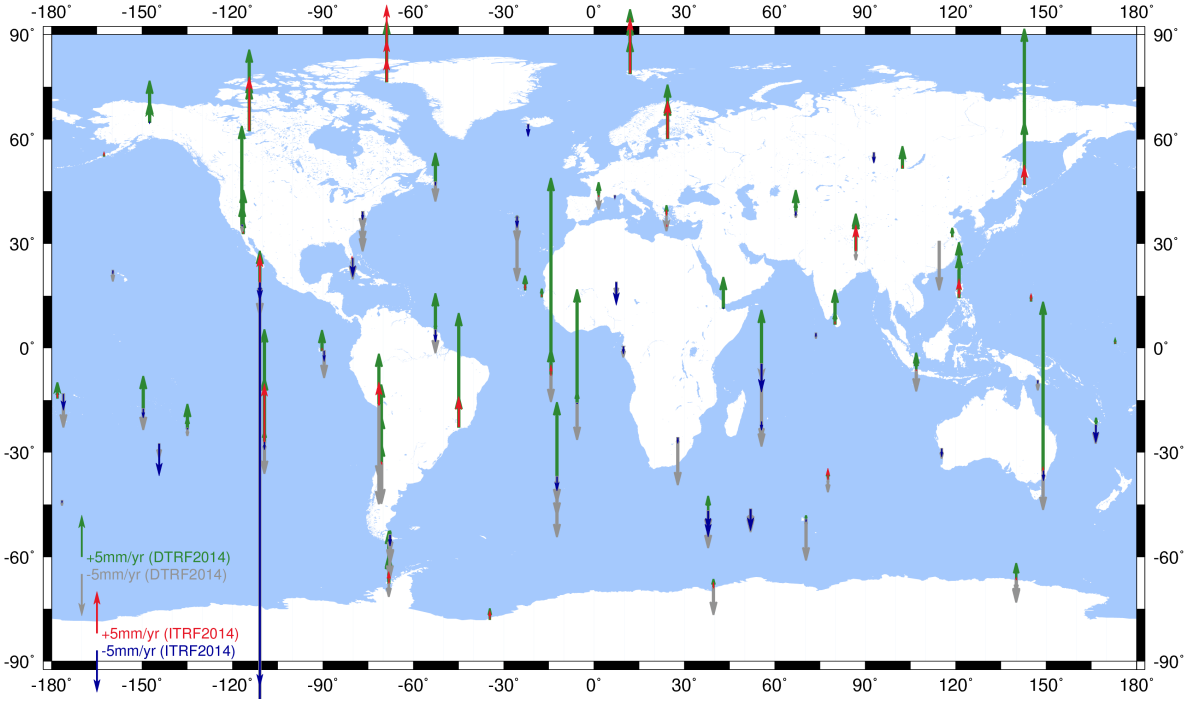

Fig. 2: *Vertical DORIS velocities from DTRF2014 and ITRF2014.*

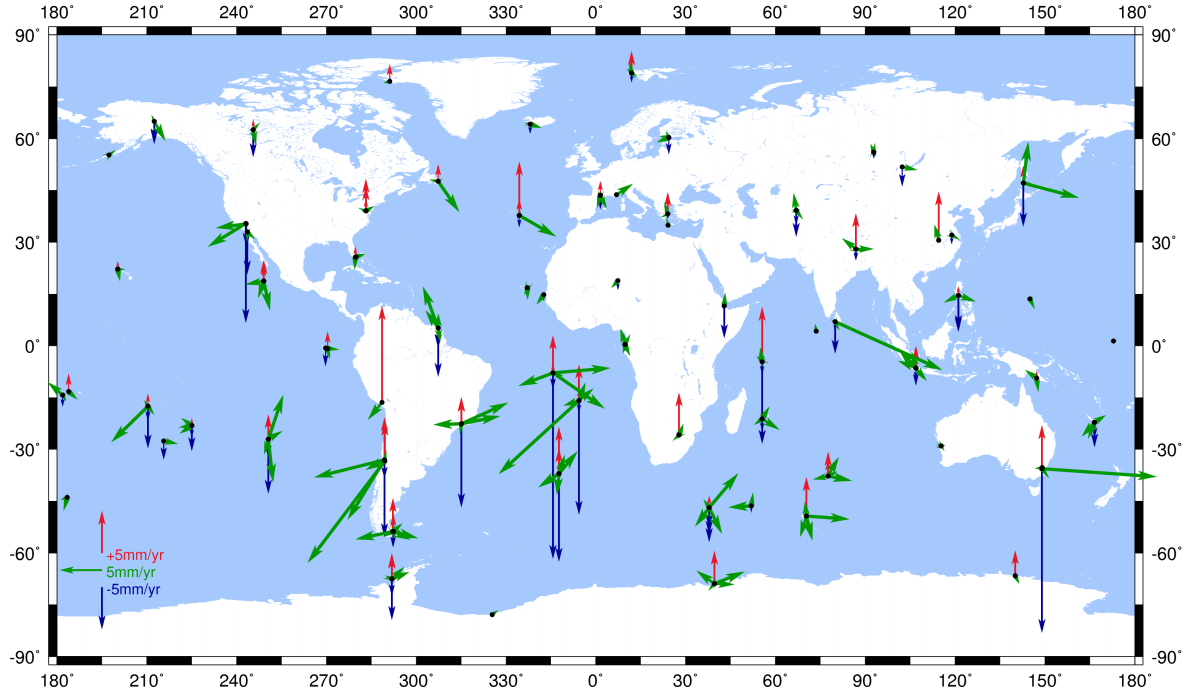

Fig. 3: *Velocity differences between DTRF2014 and ITRF2014.*

Table 5: *Tie residuals of DTRF2014, ITRF2014 and JTRF2014 wrt IGN DORIS ground ties. Unit is mm.*

Datum	Nb of ties	mean	std	rms
DTRF2014	50	17	20	26
ITRF2014	50	13	13	18
JTRF2014	50	18	19	26
DTRF2014	76	20	19	28
ITRF2014	76	15	18	23

Table 6: *RMS and maxmim of station position differences between DTRF2014, ITRF2014 and JTRF2014. Unit is mm.*

Datum	Time span	East		North		Up	
		rms	max	rms	max	rms	max
DTRF2014 - ITRF2014	1993.0-2002.4	7.95	46.00	7.50	55.80	9.82	46.20
DTRF2014 - ITRF2014	2002.4-2008.5	4.01	38.00	3.24	59.90	4.97	52.40
DTRF2014 - ITRF2014	2008.5-2015.0	3.21	19.70	3.39	22.10	5.85	52.50
JTRF2014 - ITRF2014	1993.0-2002.4	7.13	32.60	6.01	42.10	13.19	47.50
JTRF2014 - ITRF2014	2002.4-2008.5	4.29	25.30	4.23	23.20	6.15	31.60
JTRF2014 - ITRF2014	2008.5-2015.0	4.82	21.00	4.16	18.80	6.60	36.20
JTRF2014 - DTRF2014	1993.0-2002.4	7.10	46.20	8.18	64.40	17.82	59.70
JTRF2014 - DTRF2014	2002.4-2008.5	4.29	23.10	4.65	21.80	7.57	23.10
JTRF2014 - DTRF2014	2008.5-2015.0	5.23	24.50	4.85	20.40	8.08	46.10

to a linear motion model as it is for DTRF2014. As a consequence, such velocity comparisons between these two solutions will have no meaning. From Fig. 3, we observe that for most of the sites with a significant velocity difference (i.e. larger than 5 mm/yr; such as Ponta-Delgada, Canberra, Santiago, St-Helena, Tristan Da Cunha), both the horizontal and vertical velocities disagree. The analysis of the velocity differences showed that they are associated with short periods of observations (smaller than 3 years) in the DTRF2014. Over the 56 position discontinuities introduced by DGFI-TUM, 31 discontinuities differ from some IGN ones by either less than seven days (frequency of the DORIS solution) or by a data gap (e.g. the DGFI-TUM discontinuity is at the start of the DORIS data gap while the IGN one is at the end), so these 31 discontinuities can be considered as in common. The JPL defined 13 DORIS position discontinuities at 10 sites; 6 discontinuities can be assimilated to ITRF2014 ones.

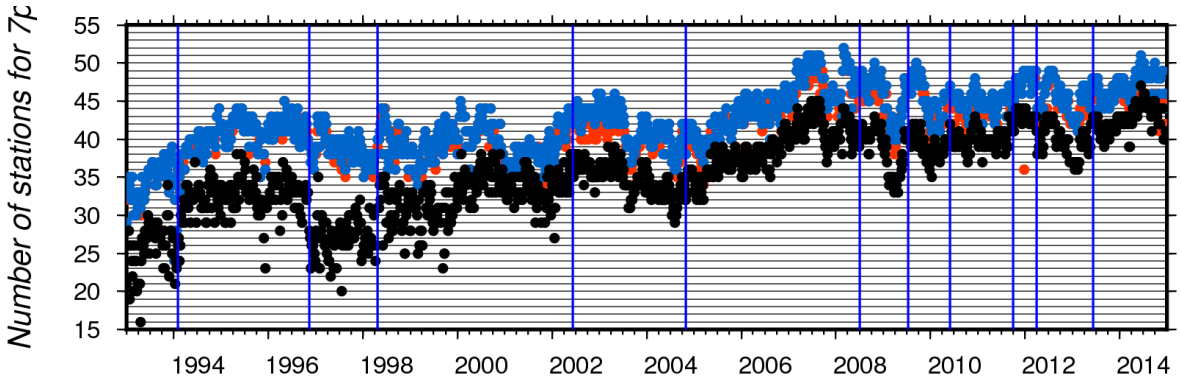

Fig. 4: *DTRF2014 (red), ITRF2014 (blue) and JTRF2014 (black) weekly DORIS network. Vertical lines correspond to DORIS satellite constellation changes.*

IDS 09 evaluation w.r.t. DTRF2014, ITRF2014, and JTRF2014

That section presents and discusses the differences in terms of Helmert parameters and station position performances while using the DTRF2014, ITRF2014, and JTRF2014 solutions as reference frame when evaluating the IDS 09 series. The software package used for the evaluation is the IGN CATREF (Combination and Analysis of Terrestrial Reference Frames) package [Altamimi *et al.*, 2002a] which was also used for the computation of the ITRF2014 solution. Each week, according to the so-called `SOLUTION/EPOCHS` of the SINEX files, we extracted the list of the active DORIS stations. Whereas in the case of JTRF2014 the positions of the active stations were simply extracted from the weekly JPL files, in the case of the DTRF2014 and ITRF2014, the weekly positions were computed from the positions and velocities given at the reference epoch. Furthermore, in the case of ITRF2014, the post-seismic corrections were taken into considerations while estimating the weekly station positions. Hereafter, by DTRF2014ntc, we denote the DTRF2014 with the atmospheric and hydrological non-tidal loading corrections and, by ITRF2014asc, the ITRF2014 within annual and semi-annual signals.

Weekly DORIS ground network

While doing the evaluation of the IDS 09 series w.r.t. the three TRF realizations (DTRF2014, ITRF2014, and JTRF2014), we first observed that the number of DORIS stations used to estimate the Helmert parameters w.r.t. JTRF2014 differ from the ones associated to the DTRF2014 and the ITRF2014 (see Fig. 4). The differences can be explained by a more restrictive data editing in the JPL process. From Fig. 4, we also see that the IGN networks contain more DORIS stations than the DGFI-TUM ones due to less velocity equality constraints. Using less equality constraints implies positions and velocities with larger standard deviations for stations with shorter observation time spans inducing that these stations may be rejected during the selection of the network for the Helmert parameters. To avoid any impact of the DORIS network on the Helmert parameters, in the following, we used for the evaluation the same weekly networks for the three TRFs. Each week, the network was defined as the common network between the weekly realizations of DTRF2014, ITRF2014, and JTRF2014 (see also Table 1).

Scale

As displayed in Fig. 5 and Fig. 6, the scale factors of the IDS 09 series w.r.t. DTRF2014, ITRF2014, and JTRF2014 show differences which can be associated with two time periods: before and after 2002 day-of-year (doy) 167 which corresponds to the inclusion of the DORIS missions with second generation of DORIS receivers on-board (Envisat and SPOT5). While after 2002 doy 167 the scales are very similar (in both trends and STDs – see Table 2), before that date, the scales present different trends. However, in addition to the fact that these differences

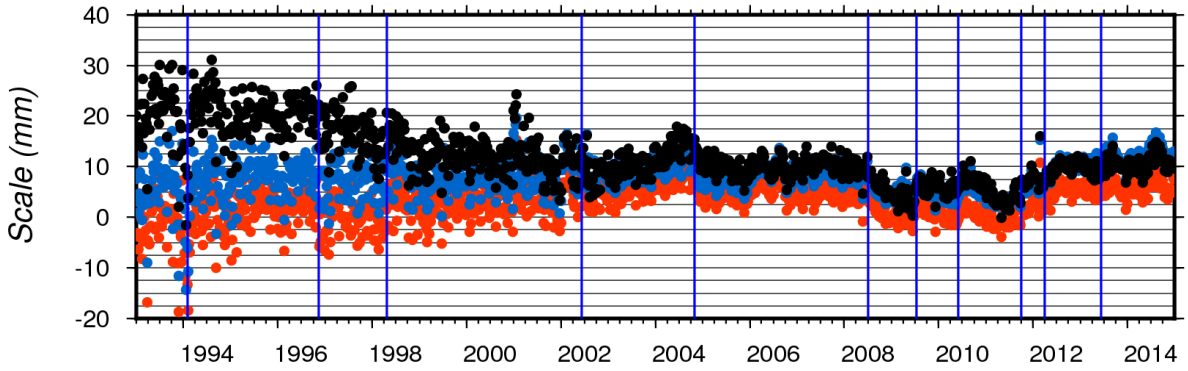

Fig. 5: *Scale factors of IDS 09 time series w.r.t. DTRF2014 (red), ITRF2014 (blue), and JTRF2014 (black). The vertical lines correspond to DORIS satellite constellation changes.*

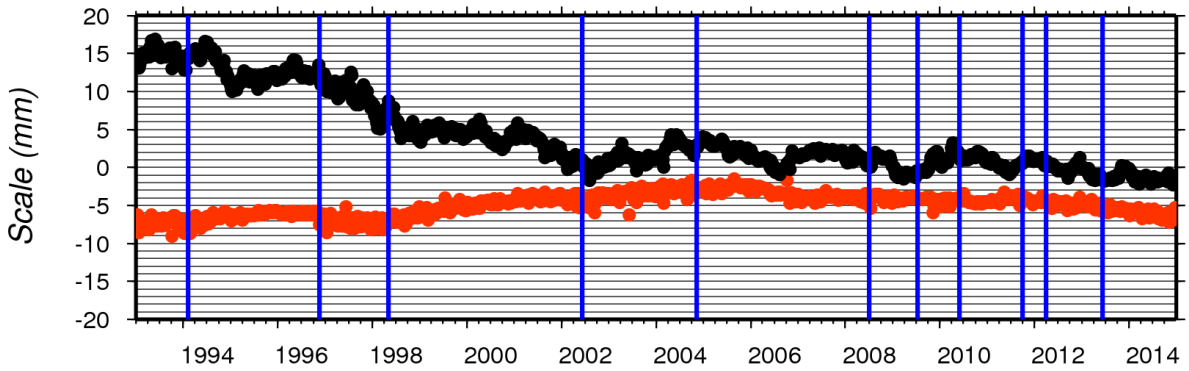

Fig. 6: *Differences of scale factors between DTRF2014 (red) and JTRF2014 (black) with ITRF2014 as seen by IDS 09 series. Vertical lines correspond to DORIS satellite constellation changes.*

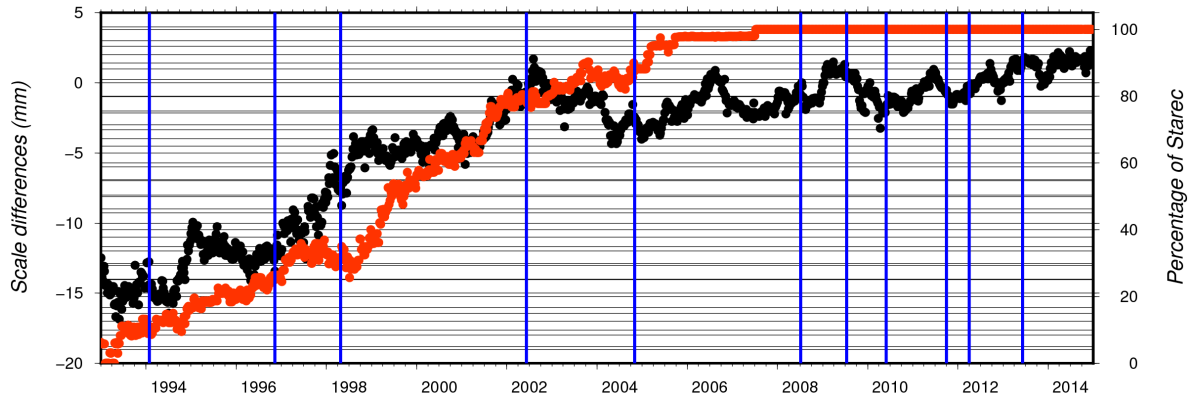

Fig. 7: *Time evolution of the scale difference between ITRF2014 and JTRF2014 (JTRF2014–ITRF2014; black) and of the percentage of STAREC DORIS ground antennas (red).*

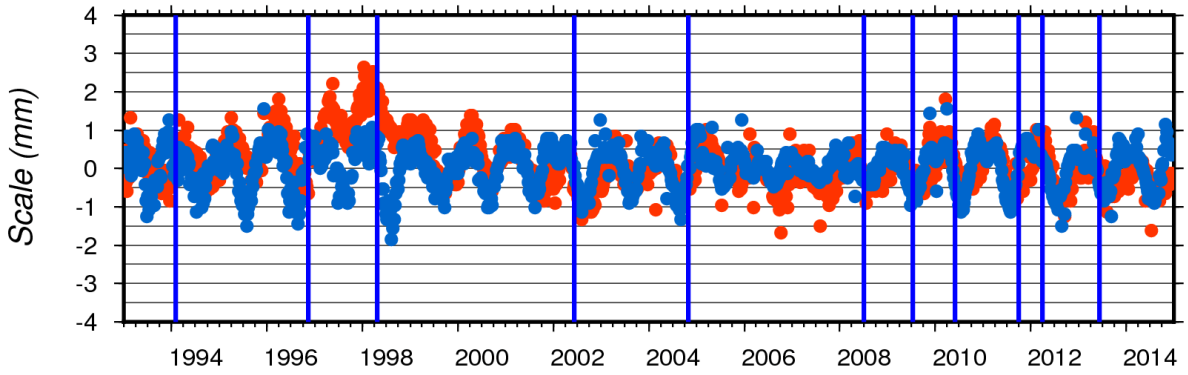

Fig. 8: *IDS 09 scale differences between DTRF2014ntc and DTRF2014 (red) and between ITRF2014asc and ITRF2014 (blue). The vertical lines correspond to the DORIS satellite constellation changes.*

occur while the DORIS constellation includes only satellite receivers of the first generation, we cannot neglect a possible correlation with the DORIS ground beacon network. As displayed in Fig. 7, until 2001, there is still a majority of ALCATEL ground antennas associated with a different phase center variation (PCV) compared to the STAREC antennas. Moreover, from that figure, we also observe a strong correlation (coefficient 0.94) between the percentage of STAREC antennas in the DORIS ground network and the scale difference between the JTRF2014 and ITRF2014 solutions. That feature must be the consequence of the different strategies the IGN and the JPL adopted to include the local ties in their processing.

From Table 2, the IGN solution gives the smallest trend whereas the JPL weekly files show the highest trend. The DTRF2014 solution provides the smallest scale offsets w.r.t. the IDS 09 solution and also shows the smallest scale trend after 2008.5. Furthermore, from Fig. 5, we also observe that the scale differences decrease after 2008 doy 195, i.e. when the missions (Jason-2, Cryosat-2, HY-2A, and Saral) with the new DGXX DORIS receiver start to be included in the IDS solution. As explained in Moreaux *et al.* [2016a] , the mean scale offsets of the IDS 09 series with the three TRF solutions are the consequence of the use of the DORIS antenna PCVs in the IDS reprocessing standards for ITRF2014.

Moreover, as pointed out by Moreaux *et al.* [2016a] , the linear pattern of the scales between 2003 doy 026 and 2004 doy 340 and between 2008 doy 244 and 2011 doy 100 is induced by the sawtooth pattern of the SPOT5-only scale see Fig. 9 from Moreaux *et al.* [2016a] . From Table 2, we also observe that the ITRF2014 gives the a constant (and stable) scale offset over the entire time span (1993.0–2015.0). In addition, as depicted by Fig. 8, the scale impact of the hydrological and atmospheric non-tidal loading corrections and of the annual and semi-annual corrections is in overall at the sub-millimeter level. The IDS 09

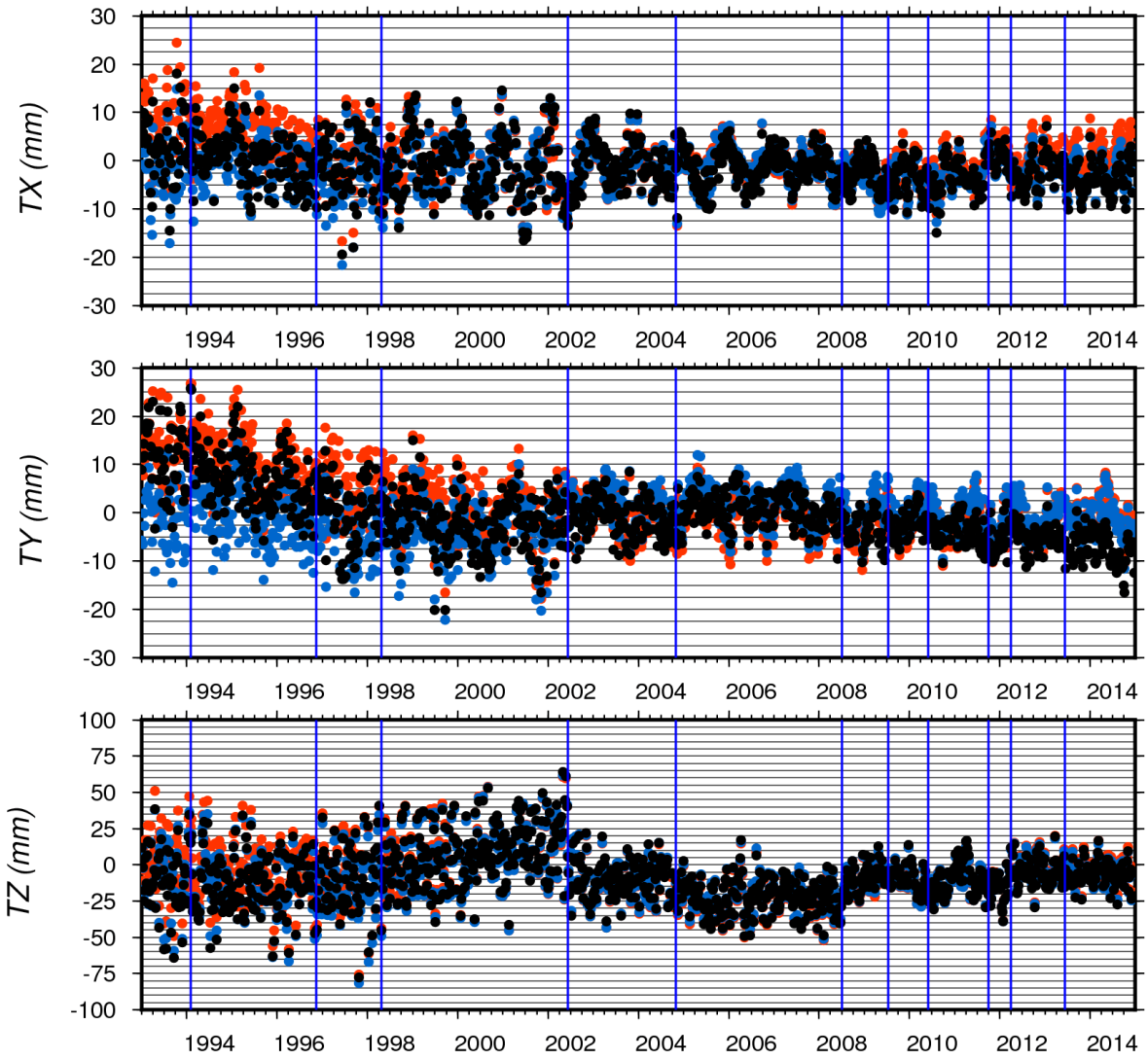

Fig. 9: *Translations of IDS 09 w.r.t. DTRF2014 (red), ITRF2014 (blue), and JTRF2014 (black). The vertical lines correspond to DORIS satellite constellation changes.*

scale differences represented in Fig. 6 may be attributable to a variety of factors, the most important of which relates the different scale definitions adopted by the three solutions. Also, tie vectors and velocity ties used to transfer the scale information from the VLBI and SLR systems to DORIS may play an important role in explaining the different temporal patterns of the scale offsets of Figure 6. Moreover, since JTRF2014 makes use of an instantaneous (and time-varying) VLBI/SLR scale definition, the values reported in Figure reflect the actual differences between the instantaneous IDS 09 and JTRF2014 scales. The mean scale offset between the DTRF2014 and the ITRF2014 solution as seen from the DORIS evaluation are about 4–5 mm which can also be clearly seen in Fig. 6.

Translations

From Fig. 9 which displays the translation parameter time series of the IDS contribution (IDS 09) to ITRF2014 w.r.t. DTRF2014 (red), ITRF2014 (blue), and JTRF2014 (black), we first observe annual signals of the x- and y-components as well as an 11 year signal on the z-translations. Furthermore, Fig. 9 shows that while the STDs of the x- and y-translation parameters are of the same order, the STDs of the z-component are 3 to 4 times larger. As early observed by Seitz *et al.* [2012], Bloßfeld *et al.* [2016b] and Moreaux *et al.* [2016a] , the z-translation is also highly correlated with the Sunspot number indicating that the DORIS z-geocenter is still suffering from a mis-modeling of the solar radiation pressure on the DORIS satellites [Gobinddass *et al.* [2010]]. Moreover, as hypothesized by Bloßfeld *et al.* [2016b], due to the strong relation between the Sunspot numbers and the atmospheric density, the IDS series may also be impacted by a problem on the atmospheric drag modeling. In addition, the T_z peak in 1999–2002 is more likely associated with activity at the peak of the solar cycle which degrades the DORIS measurements of the 800 km SPOT satellites.

From Fig. 9 and Table 2, the best compromise between the lowest trends and standard deviations of the three translations is given by ITRF2014 solution. In agreement to the scale differences, from Fig. 10, we observe that the translation differences are larger before than after 2002 doy 167. We can also see the presence of seasonal (annual and semi-annual) signal in the differences between the JTRF and ITRF translations due to the capability of the random walk to give back the station displacements induced by temporal changes of planetary fluid masses. As depicted by Fig. 11, adding atmospheric and hydrological non-tidal loading or annual and semi-annual signals on the station coordinates induce annual variations on the translation parameters with amplitudes of $\pm$4 mm peak-to-peak. It is also visible that especially in the x-component, there is a clear phase offset between the geophysical loading impact on the DTRF2014 and the artificial annual and semi-annual variations in the ITRF2014. Furthermore, according to Table 2, the use of annual and semi-annual signals from the coordinate time series within ITRF2014 allows to decrease the magnitude of the standard deviations of the translation parameters. The effect of the addition of the atmospheric and hydrological non-tidal loading corrections to DTRF2014 is mitigated: it deteriorates the T_x performances whereas it improves the mean values and standard deviations of the T_y parameter. As expected and reported in Table 4, adding the annual and semi-annual corrections to the ITRF2014 station positions reduce the amplitudes of the annual and semi-annual signals of the translation parameters.

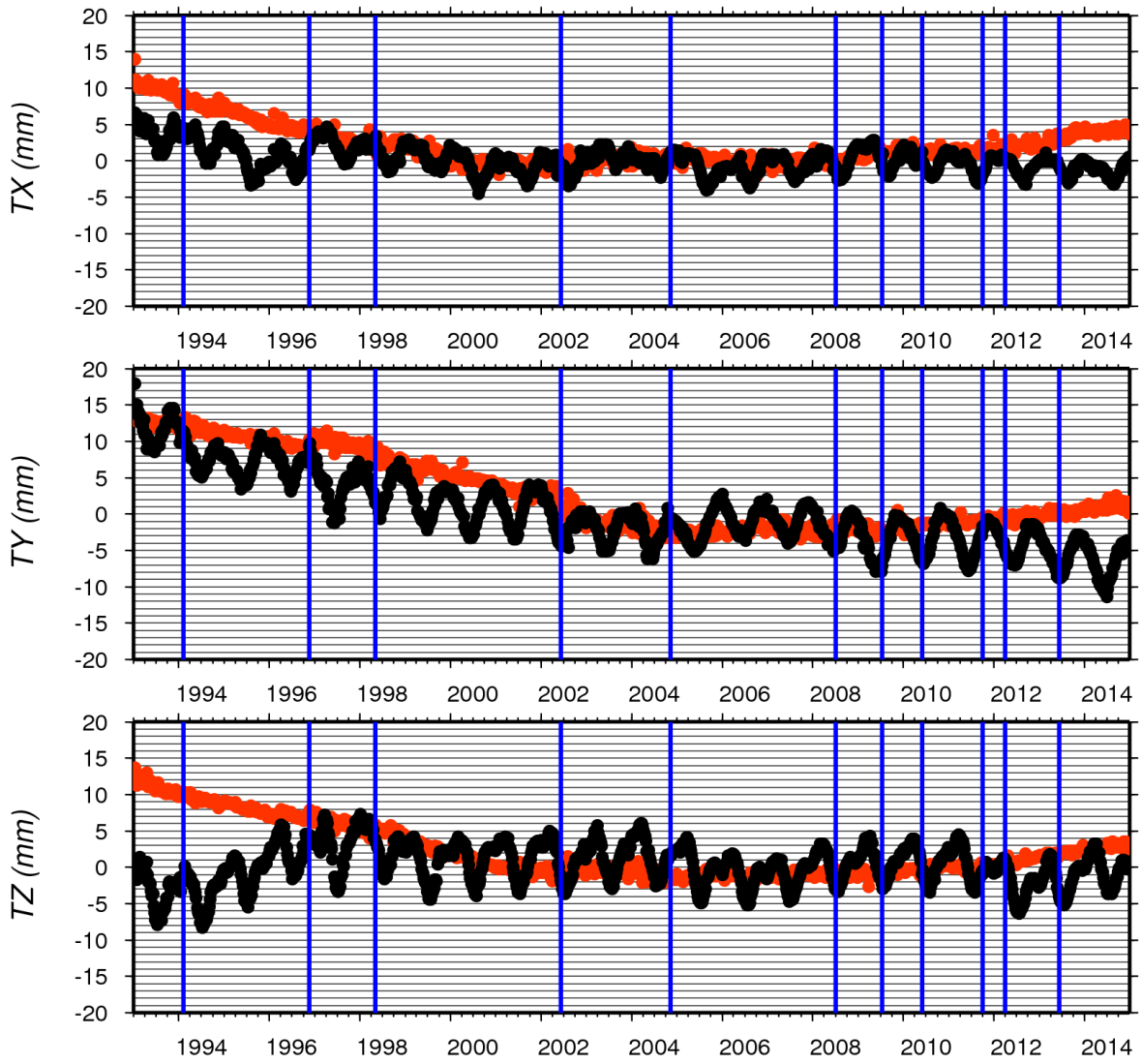

Fig. 10: *Translation differences between DTRF2014, JTRF2014 (red, black), and ITRF2014 as seen by the IDS 09 time series. The vertical lines correspond to DORIS satellite constellation changes.*

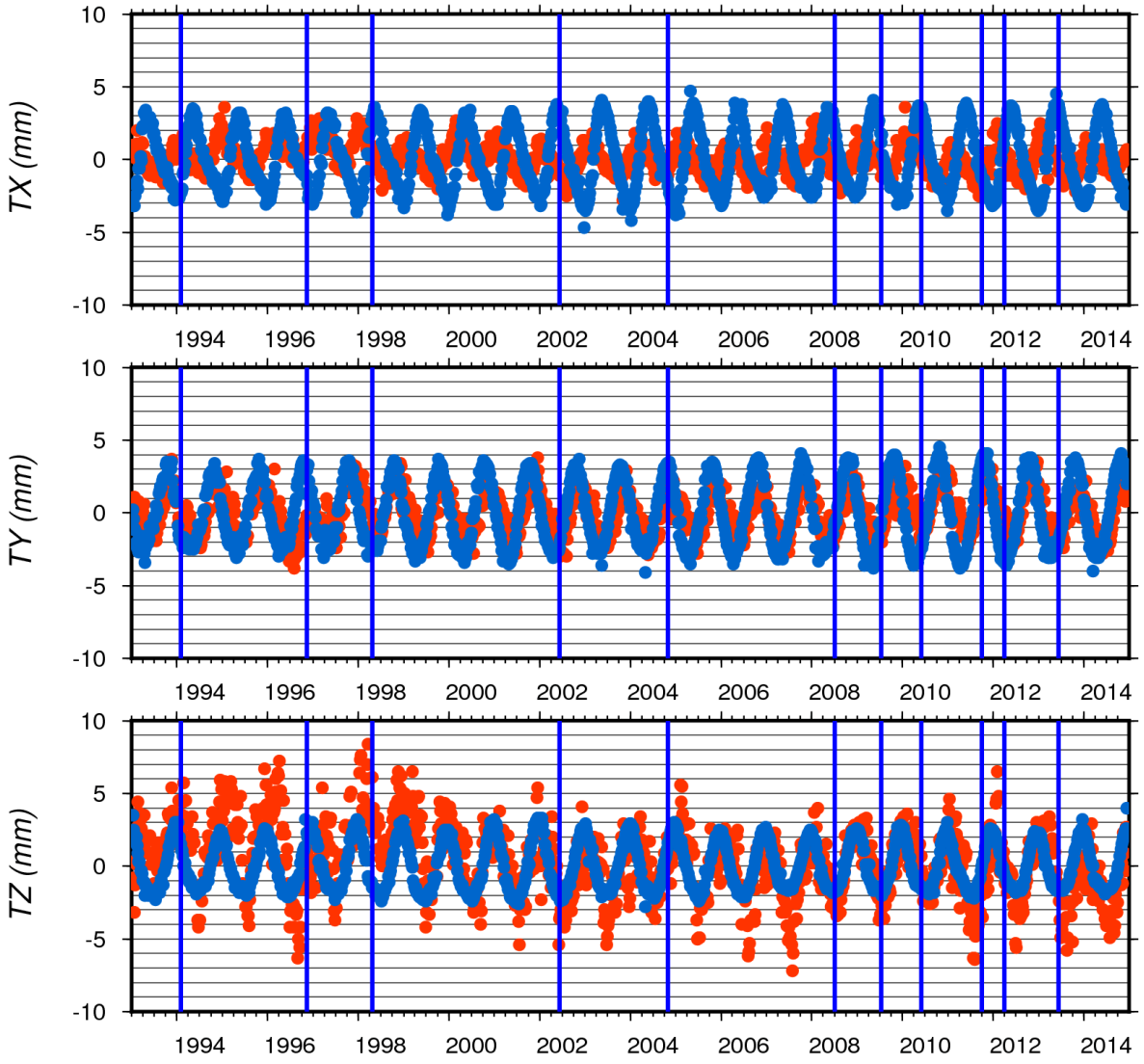

Fig. 11: *Translation differences between DTRF2014ntc and DTRF2014 (red) and between ITRF2014asc and ITRF2014 (blue) as seen by the IDS 09 time series. The vertical lines correspond to the DORIS satellite constellation changes.*

Station positioning

From the Helmert parameters, we aligned the IDS 09 series to the three TRFs and computed the WRMS (weighted RMS) of the station position residuals, i.e. differences between the aligned IDS 09 and the TRF weekly positions. From Fig. 12, we clearly see the impact of the DORIS constellation on the station positions in the local horizontal frame ENU (East, North, Up) weighted root-mean-square (WRMS) values within the three different time periods: 1993 doy 001 until 2002 doy 167, 2002 doy 188 until 2008 doy 160, and 2008 doy 188 until 2014 doy 365 which reflects the increase of the number of stations that can be tracked simultaneously on-board the DORIS satellites. The more stations being tracked, the smaller are the position WRMS expressed in the local horizontal frame. As depicted by Fig. 12, the East direction gives the worst results. This pattern is due to the fact that the Doppler technique provides observations that lack information in the direction perpendicular to the satellite track. From the three TRF solutions, even if the performances are very similar (see Table 3), we observe that slightly better results (in terms of mean and STD) are obtained using the JTRF2014 followed by the DTRF2014. This fact might be the consequence of two facts: i) the non-linear content of the JPL solution and ii) the use of the "cleaned" JPL weekly network for the Helmert parameter estimation (see Sect. Weekly DORIS ground network). However, the differences between the three TRFs expressed in NEU are less than 1.35 mm in mean and 0.15 mm in STD. Furthermore, we note no impact of the atmospheric and hydrological non-tidal loading corrections on the station position performances due to the small amplitudes of the non-tidal corrections compared to the standard-deviation of the DORIS coordinate time series. Since the non-tidal loading corrections had been computed from GNSS time series, it was assumed that DORIS beacons are affected the same way (and with the same amplitude) than GNSS antennas. Meanwhile, the including annual and semi-annual corrections in the ITRF2014 solution induces reduction of the mean WRMS in the North and Up directions by 0.15 to 0.35 mm. The impact of the annual and semi-annual corrections must be explained by larger amplitudes compared to the non-tidal ones due to the fact that these periodic signals were deduced from the coordinate time series and so, must contain not only geophysical phenomena. The RMS of the periodic corrections (resp. non-tidal corrections) are 2.92, 3.28 and 4.09 mm (resp. 0.95, 1.85, and 3.30) in ENU directions respectively. Note that Altamimi *et al.* [2016] (see Table 2) also observed that the addition of annual and semi-annual corrections gives higher improvements in the station position residuals compared to the non-tidal corrections.

Station position differences

To visualize the station coordinate differences obtained when using one of the three TRF solutions, we computed weekly DORIS station

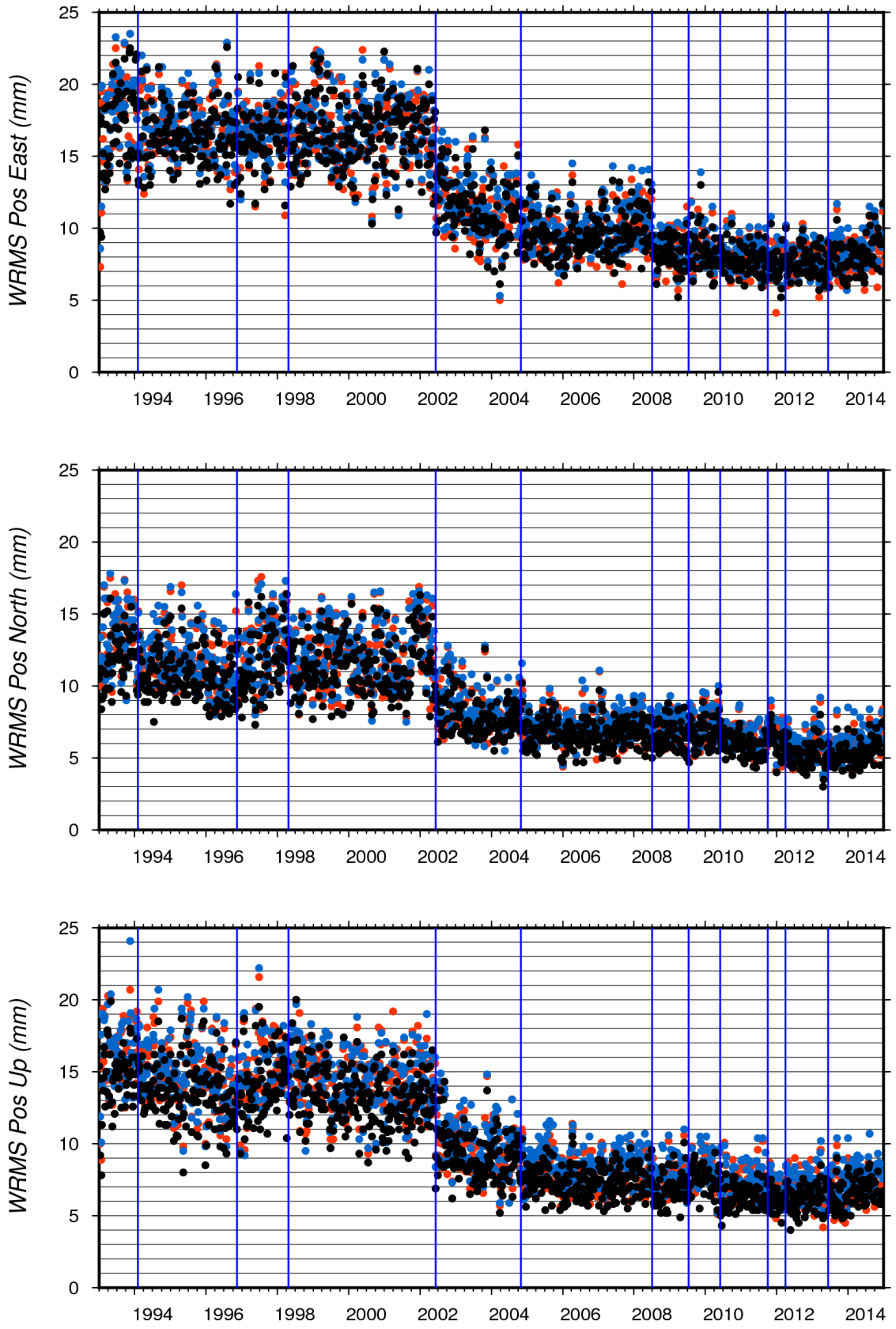

Fig. 12: *Weighted root-mean-square (WRMS) values of station positions of IDS 09 w.r.t. DTRF2014 (red), ITRF2014 (blue), and JTRF2014 (black). The vertical lines correspond to DORIS satellite constellation changes.*

networks using the positions and velocities given in the DTRF2014 and ITRF2014 SINEX files and using the weekly SINEX files of the JTRF2014. Afterwards we derived the differences between these weekly TRF solutions in the local horizontal frame (East, North, Up) of each station. In that study, we use the same ellipsoid as IDS does while generating the so-called STCD (time series of station coordinates differences) files from the DORIS weekly SINEX files. It is defined by: flattening factor 1/f=198.257810 and equatorial radius a=6378136.0 m. Due to the link between the DORIS satellite constellation and the positioning precision of the DORIS ground beacons, as we did in the previous section, we also divide the full time span into three periods: before 2002 doy 167 (first satellite of 2nd generation of DORIS receiver), 2002 doy 167 to 2008 doy 188 (first satellite with 3rd generation of DORIS receiver) and after 2008 doy 188.

The analysis of the statistics of the differences reported in Table 6, shows that i) in terms of RMS, the most important differences are on the vertical and for all the three time periods, ii) whatever is the couple of solutions, the RMS of the differences of the second and third time periods are of the same order and smaller than the RMS of the first time period; iii) point-wise, the maximum of the differences on one component can be up to 60 mm. As expected, the maximum of differences occur at a station discontinuity from one solution and so, emphasizes the differences of the discontinuity files used by the three centers. Furthermore, these maximum values are associated with either sites in seismic active zones (ex: Arequipa, Reykjavik, Santiago) or in the SAA region (ex: Cachoeira). Nevertheless, as depicted by Fig. 13, for a majority of the DORIS sites, the RMS of the 3D position differences between the three ITRF2014 realizations is smaller than 15 mm. We can also see that overall the differences between the DTRF2014 and the ITRF2014 are the smallest ones. That may be the consequence of the fact that these two solutions make the hypothesis of a linear motion (plus PSD corrections for a few sites for the ITRF2014). From that figure, the DORIS sites showing the most important differences (Arequipa, Canberra, Cachoeira, Yuzhno-Sakhalinsk, Wallis) are either sites with short time span (Canberra, Wallis) or sites in seismic active zones (Arequipa, Yuzhno-Sakhalinsk) or sites in the SAA region (Cachoeira).

Tie vector residuals

If station B supersedes to station A at a given DORIS site, we can estimate the coordinate differences between A and B from one of the ITRS realizations (at the date when B was turned on) and then, compute the difference to the tie vector from a survey (if available). This latter difference can be seen as a tie vector residual. Even if the tie residuals may reflect how the surveyed ties were used as constraints in the

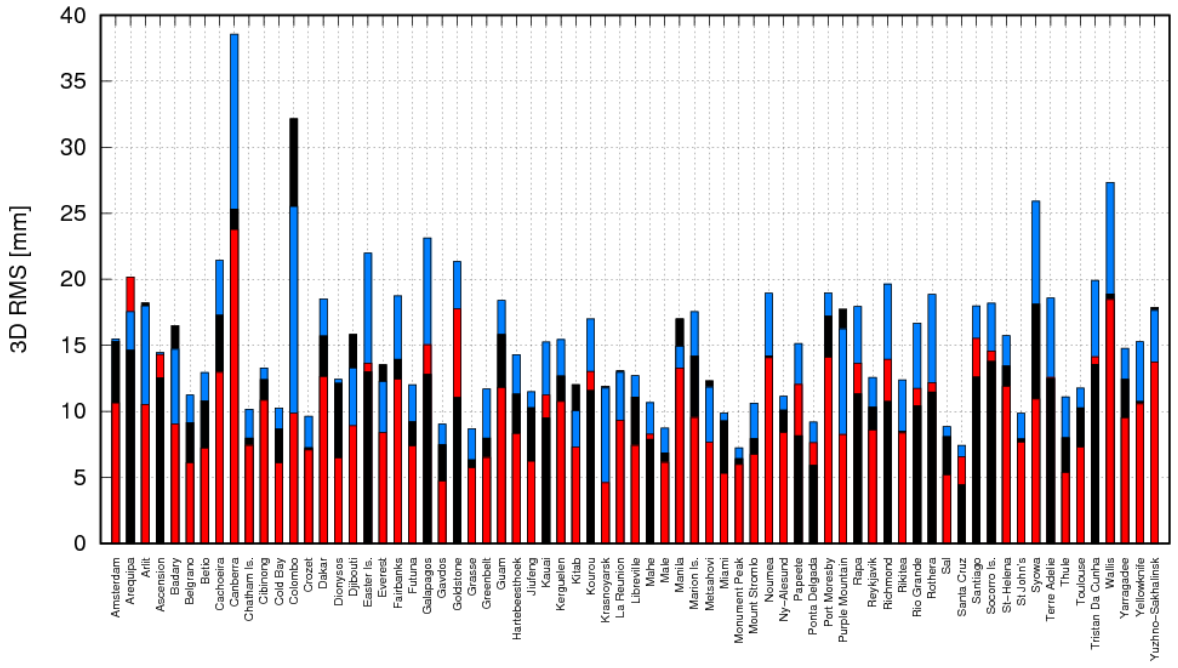

Fig. 13: *3D RMS of DORIS site coordinate time differences from 1993.0 to 2015.0 between DTRF2014, ITRF2014, and JTRF2014 (red: DTRF2014-ITRF2014, blue: JTRF2014-ITRF2014, black: JTRF2014-ITRF2014.*

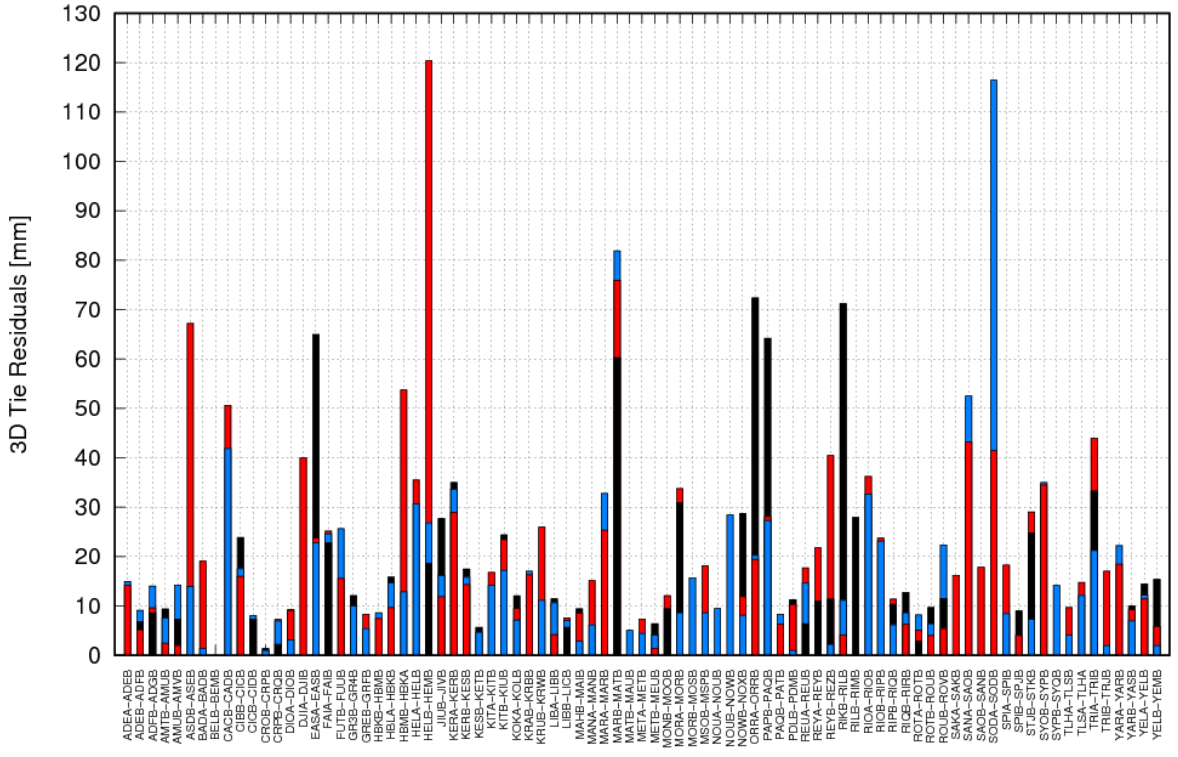

Fig. 14: *DTRF2014 (red), ITRF2014 (blue), and JTRF2014 (black) DORIS tie residuals w.r.t. the surveyed ties from IGN.*

construction of DTRF2014, ITRF2014 and JTRF2014, they can be considered as one benchmark of the quality of the three TRF solutions. Since the DGFI-TUM and IGN solutions contain velocities, it is straightforward to extrapolate the positions at any date whereas, this can not be achieved with the JTRF2014 because we only have weekly positions. Therefore, due to the amplitude of the horizontal and vertical velocities, for JTRF2014, we assumed that the ties could be obtained as the differences of the last and first weekly positions of, respectively stations A and B, if these two dates do not differ by more than one year. Thus, we end up with a set of 50 common pairs of stations between DTRF2014, ITRF2014 and JTRF2014. As depicted by Fig. 14 and reported in Table 5, the smallest differences with the surveyed ties are obtained with the ITRF2014 solution. We also observe that the DTRF2014 and JTRF2014 gives similar performances.

If we now only compare DTRF2014 and ITRF2014, due to the fact that some successive stations were separated by more than one year, we get a common set of 76 couples of stations. Once again, the IGN solution gives the smallest residuals. From Fig. 14 we can identify the stations with tie residuals larger than 50 mm: MARB-MATB and HELB-HEMB for DTRF2014, MARB-MATB for ITRF2014 and, EASA-EASB, MARB-MATB, ORRA-ORRB, PAPB-PAQB and RIKB-RILB for JTRF2014. First, we notice that the three solutions do not agree with the surveyed tie for the stations MARB and MATB at Marion Island in the Southern Indian ocean. According to Moreaux *et al.* [2016b], that discrepancy may be the consequence of the South Africa earthquake of magnitude 5.4 which happened in 2002, June 16. Second, the DTRF2014 solution shows its biggest residual (121 mm) for HELB-HEMB, two stations located on the South Atlantic island of Saint-Helena. Even if that DORIS site is localized in the SAA region, as the two other ITRF realizations do not show such tie residuals, the SAA cannot be considered at the origin of the DTRF pattern. The Saint-Helena tie residual may be explained by the DTRF velocity differences between HELB and HEMB. Note that while the HEMB DTRF2014 and ITRF2014 velocities are very similar for the first period of time, the HELB velocity from DTRF2014 strongly differs than HEMB velocities as well as to HELB ITRF2014 velocity which is equal to the first velocity of HEMB (as a consequence of IGN velocity continuity constraint). Third, the length (larger than 300 days) of the time interval between the two stations must be the cause for JTRF2014 large tie discrepancies for the two station couples (ORRA-ORRB, RIKB-RILB). In the case of the couple EASA-EASB, the JTRF2014 tie discrepancy (nearly 6 mm) is the conjunction of the length of the time interval between the two stations (231 days) and the amplitude of the horizontal velocity (nearly 70 mm/yr).

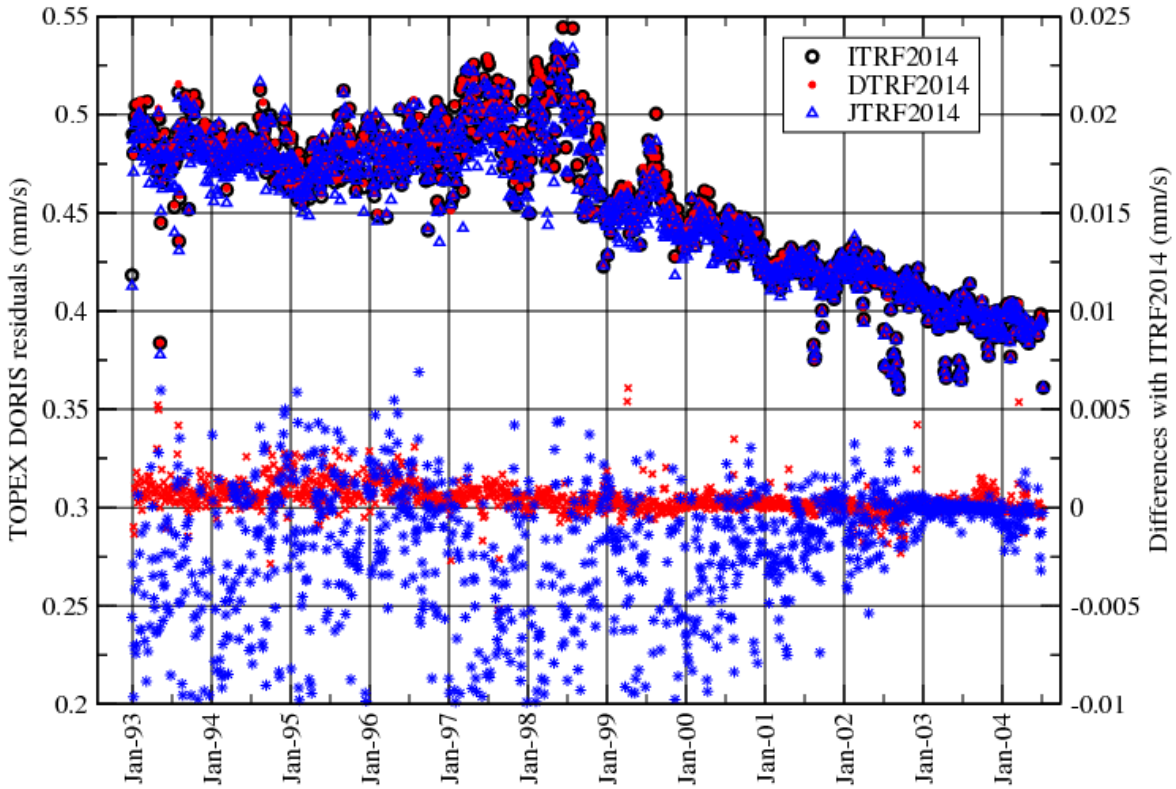

Fig. 15: *Topex DORIS RMS residuals for the DGFI-TUM, IGN, and JPL solutions and differences w.r.t. ITRF2014.*

DORIS Precise Orbit Determination Evaluation

In this section, we show the impact on selected examples of DORIS satellite orbit determination of using DTRF2014, ITRF2014 and JTRF2014 for the positioning of the DORIS ground beacons. The three realizations DTRF2014 (DGFI-TUM), ITRF2014 (IGN), and JTRF2014 (JPL) are evaluated by DORIS and SLR data processing for TOPEX, Jason-1, and Jason-2 satellites to explore the whole period of the DORIS observations. Thereby, the station coordinates of the different TRF realizations are kept fixed to see their impact on the DORIS POD. The processing of the DORIS and SLR data is performed using the GINS software [Marty *et al.*, 2011] developed by the GRGS (Groupe de Recherche de Géodésie Spatiale, i.e. the French Space Geodesy Research Group). The DORIS post-fit residuals (global and per station) and the SLR residuals on DORIS-only orbits are analyzed. We also show some orbits comparison such as the RMS of the radial differences and the mean of the z-component of the orbit differences.

POD results

This section deals with the orbit results obtained on the time span from January 03, 1993 to December 27, 2014 of Topex, Jason-1 and Jason-2 satellites for the three 2014 TRF realizations. The standards and models of the POD processing correspond to the ones used in the CNES/CLS IDS AC contribution to the IDS contribution to the ITRF2014 realization

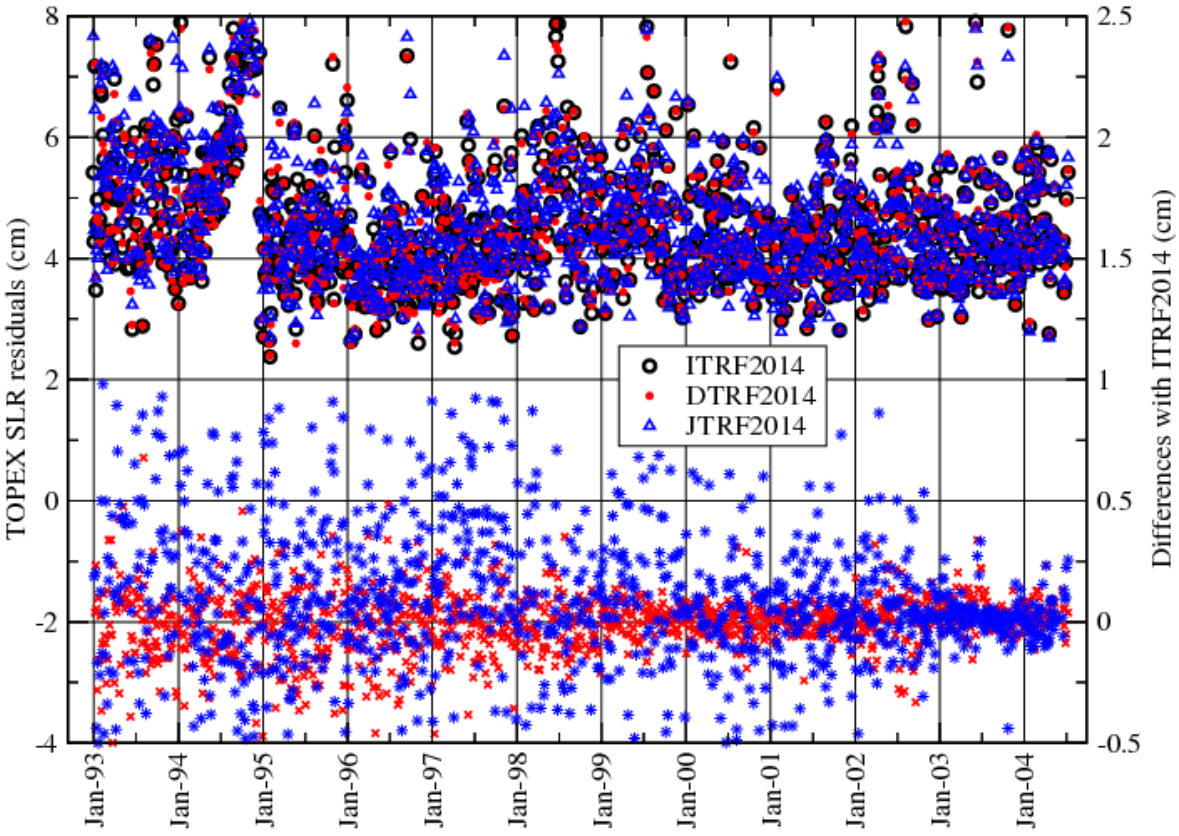

Fig. 16: *Topex DORIS-only orbit independent SLR RMS residuals for DGFI-TUM, IGN, and JPL solutions and differences w.r.t. ITRF2014.*

[Soudarin *et al.*, 2016]. Thus, Jason-1 data were corrected by the SAA corrective model from Lemoine & Capdeville [2006].

Table 7 gives the average per arc of the DORIS station number, the overall number of DORIS and SLR observations, as well as the RMS of both the DORIS and SLR residuals. For each satellite (Topex, Jason-1, Jason-2), we analyzed the differences of the DORIS RMS of fit of the orbit determination between the DTRF2014, the JTRF2014, and the ITRF2014 solution. The DORIS-only orbits were also evaluated by independent SLR data processing. Then, we focused on the differences of the RMS of the DORIS residuals per station. Due to a more aggressive data editing of the JPL solution, compared to the DTRF2014 and ITRF2014, the weekly JTRF2014 files contain less stations, particularly at the beginning of the processed time period. After the end of 2014, there are fewer stations for the ITRF2014 and DTRF2014 solutions because the new DORIS stations were not part of the IDS contribution to ITRF2014, and so not in the ITRF solutions. As a consequence, we decided to make the comparisons until the end of 2014.

To analyze the impact of the different 2014 TRF realizations on the DORIS residuals, we looked at the differences between the ITRF2014 and the two other 2014 TRF solutions. When the differences are positive, the ITRF2014 solution is better than the two others solutions. The fact that the JTRF2014 contains fewer stations at the beginning of the processed period may also explain the best performances of the JTRF2014 solution in terms of DORIS RMS residuals (see Table 7 and Fig. 15). According to Table 7 and Fig. 15, the DTRF2014 and ITRF2014 solutions give very similar DORIS RMS residuals. Nevertheless, as depicted by Fig. 15, the DTRF2014 performs slightly less well than ITRF2014 before January 1999. We also analyzed the DORIS RMS residual differences per station between the three TRF solutions. For these calculations, in order to not bias the results, we took into account exactly the same observations. The results show that the three solutions are very close. Meanwhile, the JTRF2014 gives the best results probably thanks to a reduction of the observations number and to the Kalman capability to capture more than the secular variations of the DORIS station positions. To evaluate the quality of the different 2014 TRF realizations, we also estimated the SLR residuals on the DORIS-only orbits. For Topex, even if the overall DORIS RMS residuals are lower (explained above), the JTRF2014 solution gives the worst SLR RMS residuals. That's the consequence of the lower number of SLR points associated to the JTRF2014 (see Table 7 and Fig. 16). We can see also from mid 2002, when the observations number is similar, that the JTRF2014 solution is equivalent to the two others. The DGFI and IGN solutions are very similar and give the same global RMS residuals value of 4.58 cm.

For Jason-1, as shown in Table 7 and Fig. 17, the three solutions i) are very close in terms of DORIS and SLR RMS residuals and ii) give the same global DORIS RMS residuals (0.307 mm/s). Furthermore, we observe that the DTRF2014 solution shows slight improvements (about 0.5 %) over one period of 7 months (from August 2004 to February 2005). That improvement can be directly correlated to the smaller number of observations (stations) during this time span. It also explains why the RMS residuals per station are systematically lower, except for about ten stations in the case the DTRF2014 solution compared to the ITRF2014. However, the DTRF2014 shows slight, but systematically lower, DORIS residuals for Jason-1 than the ITRF2014. Note that for Yuzhno-Sakhalinsk (SAKA) and Rapa (RAQB) stations, the results are not significant because it concerns only very few arcs. Regarding the JTRF2014 solution, there are two periods: a degradation from January to March 2006 and, an improvement from May to September 2008. These two periods are associated to a reduction of the observations number. Every time the observations number is similar, the three solutions give roughly the same DORIS RMS residuals. With regard to Jason-2, as shown in Table 7, in Fig. 19 and in Fig. 20, the three solutions are also very similar in terms of DORIS and SLR RMS residuals. However, there are two periods where the DTRF2014 solution is slightly worse than the ITRF2014 (<0.5 %): from February 2010 to January 2011 and after May 2014. The degradation for the first period is explained by the high RMS residuals obtained for the Santiago station (SANB). The second period corresponds to fewer observations (up to 4 stations less) for DTRF2014.

One important fact to note is that the differences between all the 2014 TRF solutions are at a very low level, in particular for the Jason-1 and Jason-2 (see Table 7). The JTRF2014 solution looks better but there are fewer observations and some missing stations. It is also a weekly solution and it cannot be usable in prediction. For these reasons, the ITRF2014 solution presents the best overall performances.

Table 7: *Summary of POD results.*

DORIS mission	TRF Solution	# DORIS points (mean)	# DORIS points (mean)	# SLR points (mean)	RMS residuals DORIS [mm/s]	RMS residuals SLR [cm]
TOPEX	ITRF2014	39.8	18,718	1,662	0.455	4.58
	DTRF2014	39.8	18,765	1,663	0.456	4.58
	JTRF2014	35.3	17,226	1,665	0.452	4.69
Jason-1	ITRF2014	43.9	36,270	1,463	0.307	2.52
	DTRF2014	43.8	36,106	1,463	0.307	2.51
	JTRF2014	43.2	35,913	1,464	0.307	2.53
Jason-2	ITRF2014	46.3	50,934	1,646	0.313	2.15
	DTRF2014	45.9	50,498	1,645	0.313	2.17
	JTRF2014	45.7	50,458	1,648	0.312	2.15

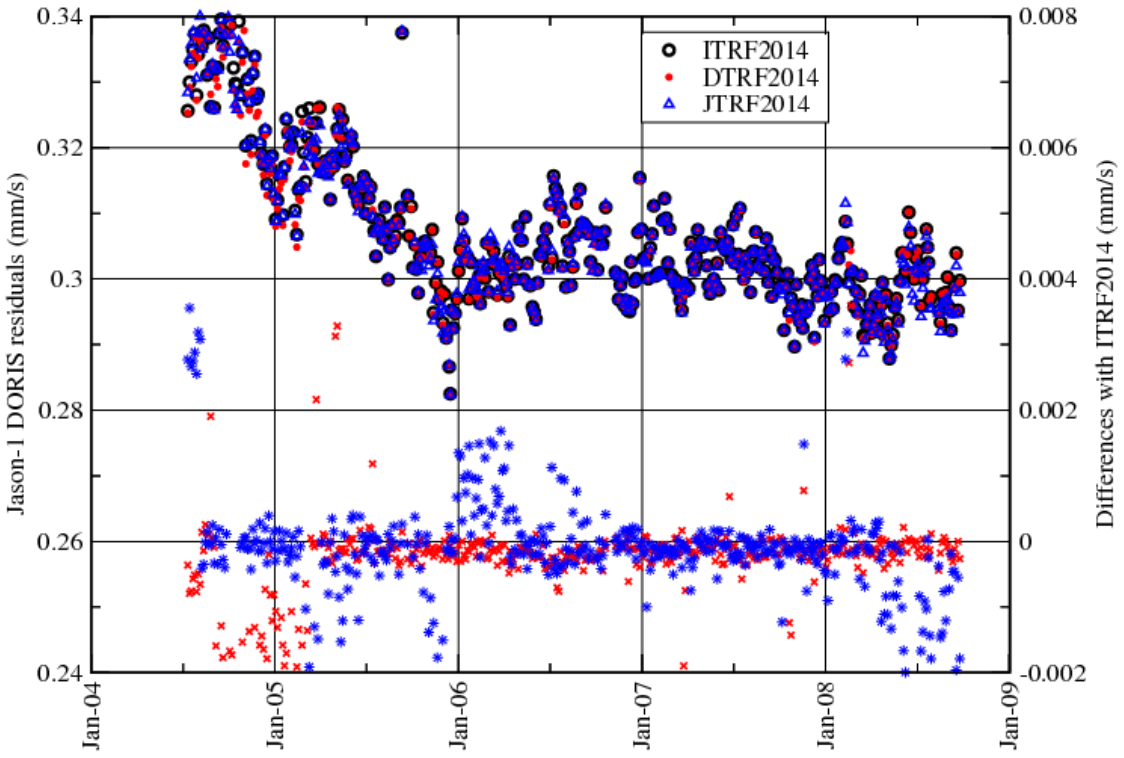

Fig. 17: *Jason-1 DORIS RMS residuals for the DGFI-TUM, IGN, and JPL solutions and differences w.r.t. ITRF2014.*

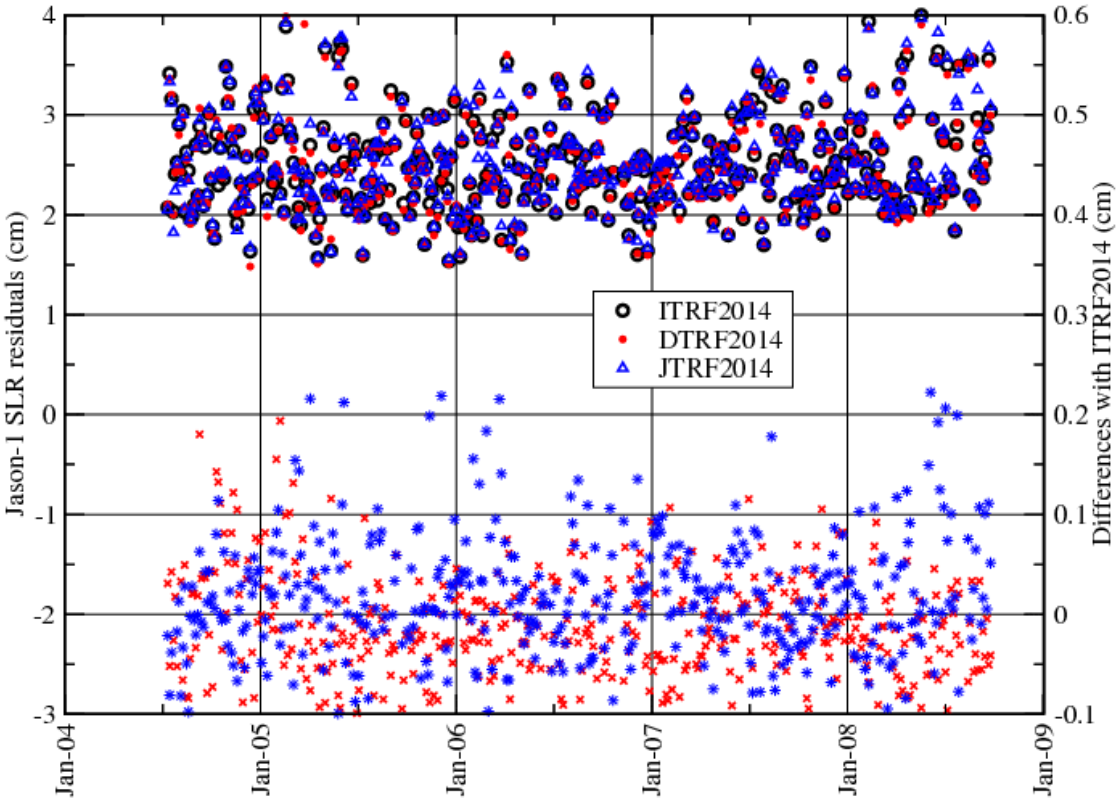

Fig. 18: *Jason-1 DORIS-only orbit independent SLR RMS residuals for DGFI-TUM, IGN, and JPL solutions and differences w.r.t. ITRF2014.*

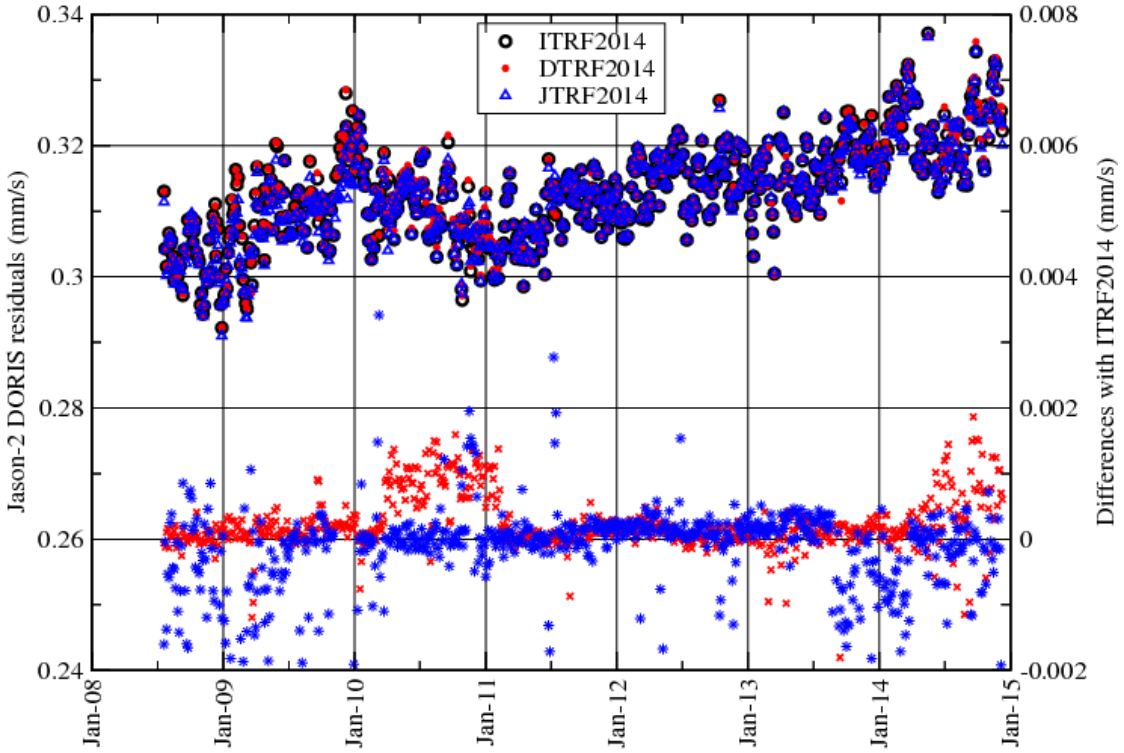

Fig. 19: *Jason-2 DORIS RMS residuals for the DGFI-TUM, IGN, and JPL solutions and differences w.r.t. ITRF2014.*

Orbital z-differences

Fig. 21 gives the orbit centering difference in the z-direction. We observe i) an important drift of DTRF2014 w.r.t. ITRF2014 from 1993 to 2001; ii) a 2 mm bias of DTRF2014 w.r.t. ITRF2014 from February 2010 to January 2011 as a consequence of a different positioning of the Santiago station; iii) an annual signal for the JTRF2014 realization. The annual signal markedly visible in the JTRF2014 solution can also be found in the time series of the translation offsets of JTRF2014 to ITRF2014 (see Fig. 9) and mostly attributable to the sub-secular nature of JTRF2014.

The drift of the DTRF2014 solution from 1993 to 2001 can also be correlated to the difference of the z-translation between the DTRF2014 and ITRF2014 solutions displayed by the Fig. 9 (around 10 mm from 1993 to 2001). Similarly to the results obtained on the mean z-differences, as depicted by Fig. 22, the RMS of the radial orbit differences between DTRF2014 (resp. JTRF2014) and ITRF2014 show an important drift from 1993 to 2001 (resp. an annual signal). The dispersion and the level of the RMS are higher (and different) between 1993 and 2002 for the TRF solutions. After 2003, the level of RMSfor the three 2014 TRF realizations is more consistent. These results can be correlated to the scale factors of IDS 09 w.r.t. 2014 TRF solutions depicted by the Fig. 5.

As explained in Sect. Scale, the change after mid of 2004 (resp. mid of 2008) can been explained by the including of the DORIS missions with on-board the second (resp. third) generation of DORIS receivers starting with with Jason-1 (resp. Jason-2).

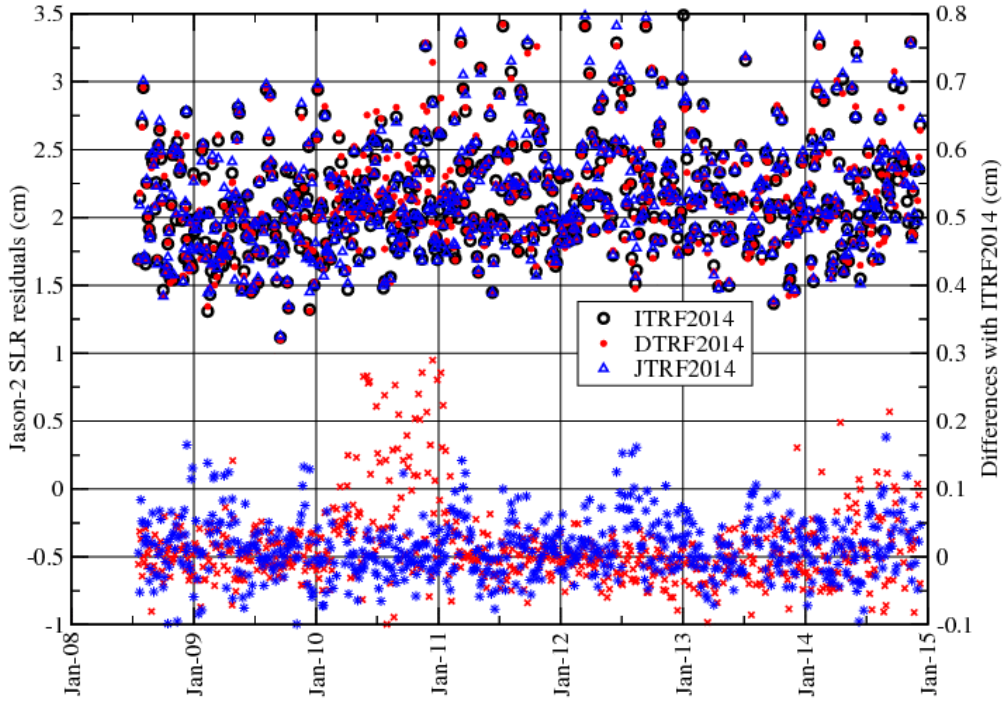

Fig. 20: *Jason-2 DORIS-only orbit independent SLR RMS residuals for DGFI-TUM, IGN, and JPL solutions and differences w.r.t. ITRF2014.*

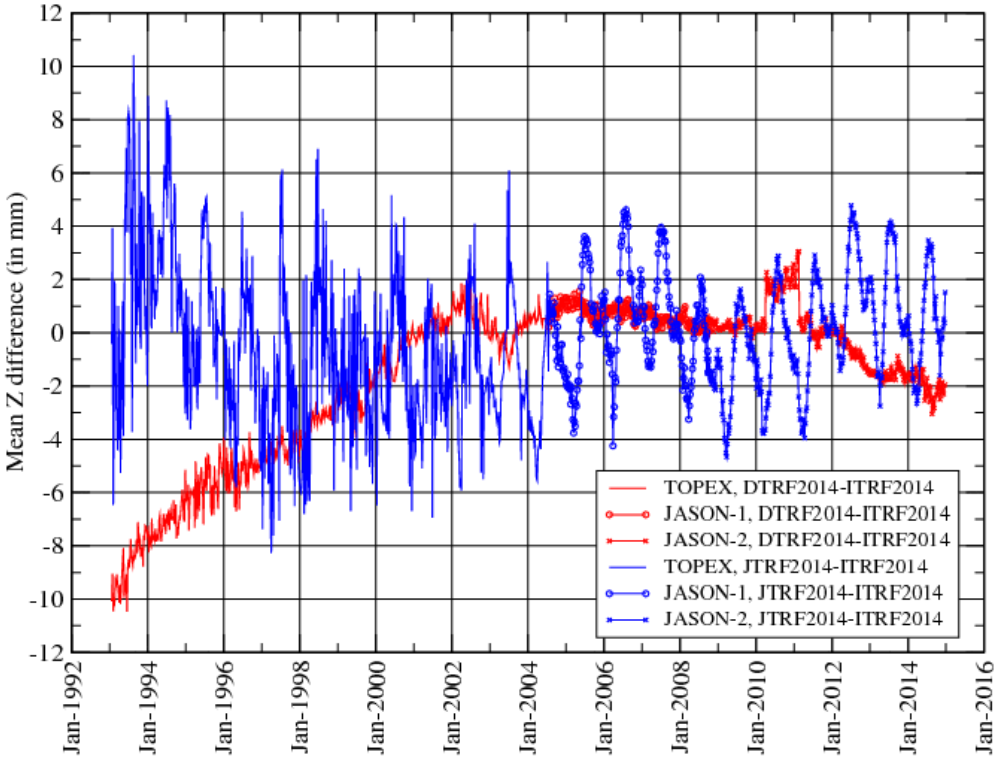

Fig. 21: *Mean orbital z-differences between DGFI-TUM, IGN, and JPL solutions.*

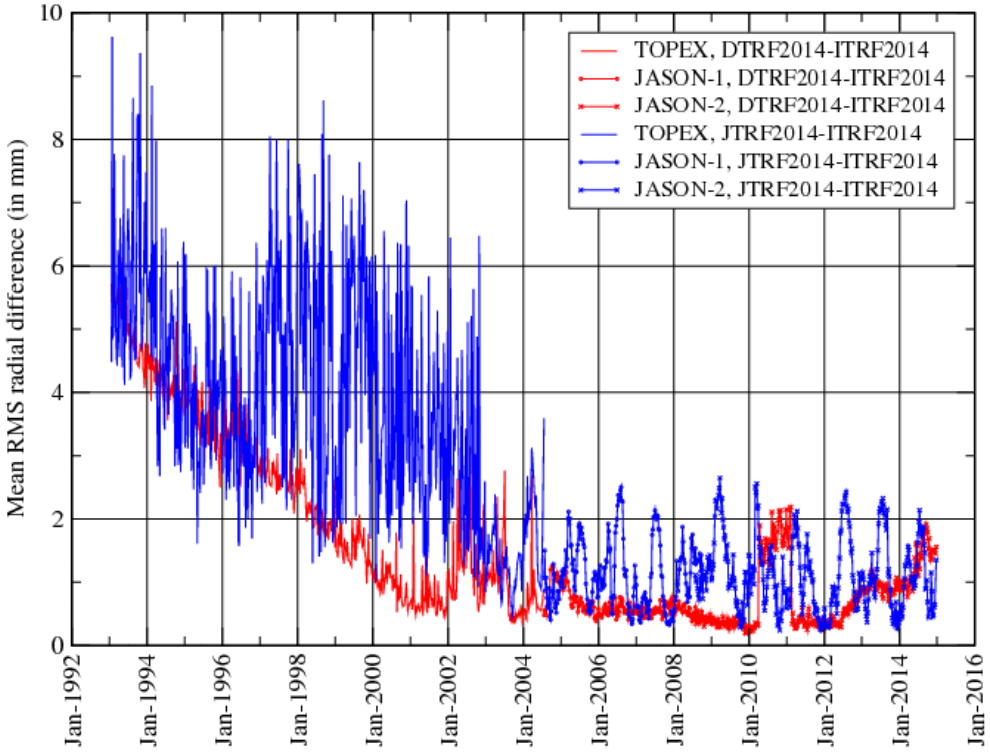

Fig. 22: *RMS of orbital z-differences (radial) between DGFI-TUM, IGN, and JPL solutions.*

Conclusions

This paper evaluates the DORIS component of the three 2014 TRF realizations: DTRF2014 from DGFI-TUM, ITRF2014 from IGN, and JTRF2014 from JPL. After a brief presentation of the methodology of the computation of the three solutions, the solution SINEX files are analyzed. That first analysis shows that i) due to a more intensive data editing, the weekly SINEX files from the JPL contain less DORIS stations than the two cumulative solutions from DGFI-TUM and IGN; ii) as the consequence of the use of velocity constraints to force the same value over multiple segments (unless a velocity discontinuity was observed) and iii) the DORIS stations showing large velocity differences (i.e. larger than 5 mm/yr) between DTRF2014 and ITRF2014 were stations with a short period of observations.

Then, we estimate, compare and analyze the Helmert transformation parameters of the IDS 09 series [IDS contribution to ITRF2014, Moreaux *et al.*, 2016a] w.r.t. the three 2014 TRF realizations as well as w.r.t. the DGFI-TUM solution including atmospheric and hydrological non-tidal loading and the IGN solution including annual and semi-annual station position corrections. The scale and translation parameter time series (see Fig. 5 and Fig. 9) show a better agreement after mid of 2002 and the addition of the first missions (Envisat, SPOT5) with on-board the second generation of DORIS receiver. Furthermore, while the DGFI-TUM scale differs to the IGN scale by at most 5-10 mm (see Fig. 6), the differences between the JPL and IGN scales can reach 10-15 mm between 1993.0 and 1998.3 (the including of SPOT4). Nevertheless, the DGFI-TUM scale agrees better (in case of the overall offset) to the IDS 09 solution than the other two TRF solutions do. As depicted by Fig. 7, the correlation between the difference of the JPL and the IGN scales and the percentage of STAREC antennas in the ground network suggests that the scale difference may be the consequence of the different strategies IGN and JPL adopted while including the local ties. In terms of Helmert parameters, the impact of the including of either atmospheric and hydrological non-tidal corrections or annual and semi-annual corrections is very limited. In overall, we observe that the IGN solution gives the more stable transformation parameters over the full time span (1993.0–2015.0, see Table 2), but the DTRF2014 shows the smallest scale offsets w.r.t. the IDS 09 time series. As expected, due to the capability of the random walk to give back the station displacements by temporal changes of planetary fluid masses, the JTRF2014 gives the best performances in terms of station position residuals (see Table 3). The analysis of the station position residuals also shows a better improvement of the including of the annual and semi-annual corrections compared to addition atmospheric and hydrological non-tidal corrections thanks to larger amplitudes of the former corrections and to the fact they must contain more than the geophysical phenomena.

In addition to the translation and the scale parameter time series, we also discussed the impact of using these three 2014 TRF realizations in the positioning of the DORIS stations. That test consisted in estimating the East, North, and Up weekly positions of the DORIS stations from the three solutions over the full time span (1993.0–2015.0). As revealed by Table 6, the RMS of the horizontal position differences are smaller than 10 mm whereas the RMS of the vertical discrepancies are smaller than 20 mm. The differences in the height component are fully correlated with the scale differences. The investigation on the maximum values showed that these were point values corresponding to i) dates of discontinuities in one of the solutions and ii) to stations located in either seismic zones (ex: Arequipa, Reykjavik, Santiago) or SAA region (ex: Cachoeira). The analysis of the site-by-site 3D RMS coordinate differences (see Fig. 13) showed that the most important values were also in seismic or SAA regions as well as associated with short period of observations. In addition to the station position differences, to evaluate the DTRF2014, ITRF2014 and JTRF2014 solutions, we analyzed the discrepancies between the estimated (from the solutions) and measured (from the IGN leveling team) DORIS tie vectors. That study illuminated the best results from the ITRF2014.

An additional issue of concern is the impact of these three 2014 TRF realizations in the framework of DORIS POD. As showed in Sect. POD results, the differences between the three solutions are at a very low level, in particular for the Jason-1 and Jason-2 results. For the ITRF2014 and DTRF2014 solutions, the most significant improvements are obtained for the time periods from 1992 to 1998 and from 2010 to 2014. That may be due to the improvement of the estimation of the station velocities compared to those estimated in the DPOD2008 solution. The POD evaluation of the ITRF2014 solution including annual and semi-annual corrections and the DTRF2014 solution including atmospheric and hydrological non-tidal loading revealed no significant impact.

In summary, based on the different criteria used for evaluation, even if the three solutions gives similar results in terms of DORIS positioning and DPOD POD, we showed that it is the ITRF2014 solution from IGN which presents the best overall performances. As a consequence, we recommend it as the standard and the reference for future IDS products. It should be pointed out here again, that this investigation of the ITRF2014 solution was only possible since several solutions had been computed for the most recent ITRF realization. This study emphasizes the need for multiple solutions to inter-compare and validate results.

Acknowledgements

Part of this work was performed at CLS under contract with the Centre National d'Etudes Spatiales (CNES). Part of this work was carried out at

the Jet Propulsion Laboratory – California Institute of Technology, under a contract with the National Aeronautics and Space Administration (NASA).

References

Abbondanza C., Chin T.M., Gross R., *et al.* (2017) JTRF2014, the JPL Kalman Filter and Smoother Realization of the International Terrestrial Reference System. J Geophys Res, DOI 10.1002/2017JB014360

Altamimi Z., Boucher C., Sillard P. (2002a) New trends for the realization of the international terrestrial reference system. Adv Space Res, vol 30(2), pp 175–184, DOI 10.1016/S0273-1177(02)00282-X

Altamimi Z., Collilieux X., Legrand J., *et al.* (2007) ITRF2005: a new release of the International Terrestrial Reference Frame based on time series of station positions and earth orientation parameters. J Geophys Res, vol 112(B9), B09401, DOI 10.1029/2007JB004949

Altamimi Z., Collilieux X. & Métivier L. (2011) ITRF2008: an improved solution of the international terrestrial reference frame. J Geod, vol 85(8), pp 457–473, DOI 10.1007/s00190-011-0444-4

Altamimi Z., Rebischung P., Metivier P., *et al.* (2016) ITRF2014: A new release of the International Terrestrial Reference Frame modeling non-linear station motions. J Geophys Res, vol 121(8), pp 6109–6131, DOI 10.1002/2016JB013098

Bloßfeld M., Seitz M., Angermann D. (2014) Non-linear station motions in epoch and multi-year reference frames. J Geod, vol 88(1), pp 45–63, Springer, DOI 10.1007/s00190-013-0668-6

Bloßfeld M., Seitz M., Angermann D. (2016a) Epoch reference frames as short-term realizations of the ITRS – datum stability versus sampling. IAG Symposia 143, Springer Berlin Heidelberg, pp 26–32, DOI 10.1007/1345_2015_91

Bloßfeld M., Seitz M., Angermann D., *et al.* (2016b) Quality assessment of IDS contribution to ITRF2014 performed by DGFI-TUM. Adv Space Res, vol 58(12), pp 2505–2519, DOI 10.1016.j.asr.2015.12.016

Capdeville H., Štěpánek P., Lemoine J.-M., *et al.* (2016) Update of the corrective model for Jason-1 DORIS data in relation to the South Atlantic Anomaly and a corrective model for Spot-5. Adv Space Res, vol 58(12), pp 2628–2650, DOI 10.1016/j.asr.2016.02.009

Gobinddass M. L., Willis P., Menvielle M., *et al.* (2010) Refining DORIS atmospheric drag estimation in preparation of ITRF2008. Adv Space Res, vol 46(12), pp 1566–1577, DOI 10.1016/j.asr.2010.04.004

Lemoine J.-M. & Capdeville H. (2006) A corrective model for Jason-1 DORIS Doppler data in relation to the South Atlantic Anomaly. J Geod, vol 80(8-11), pp 507–523, DOI 10.1007/s00190-006-0068-2

Marty J. C., Loyer S., Perosanz F., *et al.* (2011) GINS: the CNES/GRGS GNSS scientific software, 3rd International Colloquium Scientific and Fundamental Aspects of the Galileo Programme, ESA Proceedings WPP326, 31 August – 2 September 2011, Copenhagen, Denmark.

Moreaux G., Lemoine F. G., Capdeville H., *et al.* (2016a) The International DORIS Service contribution to the 2014 realization of the International Terrestrial Reference Frame. Adv Space Res, vol 58(12), pp 2479–2504, DOI 10.1016/j.asr.2015.12.021

Moreaux G., Lemoine F. G., Argus D. F., *et al.* (2016b) Horizontal and vertical velocities derived from the IDS contribution to ITRF2014, and comparisons with geophysical models. Geophys J Int, vol 207, pp 209–227, DOI 10.1093/gji/ggw265

Rudenko S., Dettmering D., Esselborn S., *et al.* (2014) Influence of time variable geopotential models on precise orbits of altimetry satellites, global and regional mean sea level trends. Adv Space Res, vol 54(1), pp 92–118, DOI 10.1016/j.jog.2014.04.008

Rudenko S., Bloßfeld M., Müller H., Dettmering D., Angermann D., Seitz M. (2017) Evaluation of DFTR2014, ITRF2014 and JTRF2014 by Precise Orbit Determination of SLR Satellites. IEEE T Geosci Remote, submitted

Saunier J. (2016) Assessment of the DORIS network monumentation. Adv Space Res, vol 58(12), pp 2725–2741, DOI 10.1016/j.asr.2016.02.026

Seitz M., Angermann D., Bloßfeld M., *et al.* (2012) The 2008 DGFI realization of the ITRS: DTRF2008. J Geod, vol 86(12), pp 1097–1123, DOI 10.1007/s00190-012-0567-2

Seitz M., Bloßfeld M., Angermann D., *et al.* (2016). The new DGFI-TUM realization of the ITRS: DTRF2014 (data). Deutsches Geodätisches Forschungsinstitut, Munich, DOI 10.1594/PANGAEA.864046 (Open Access)

Soudarin L., Capdeville H., Lemoine J. M. (2016) Activity of the CNES/CLS Analysis Center for the IDS contribution to ITRF2014. Adv Space Res, vol 58(12), pp 2543–2560, DOI 10.1016/j.asr.2016.08.006

Tourain C., Moreaux G., Auriol A., *et al.* (2016) Doris STAREC ground antennas characterization, impact on localization. Adv Space Res, vol 58(12), pp 2707–2716, DOI 10.1016/j.asr.2016.05.013

Valette J.-J., Lemoine F. G., Ferrage P., *et al.* (2010) IDS contribution to ITRF2008. Adv Space Res, vol 46(12), pp 1614–1632, DOI 10.1016/j.asr.2010.05.029

Willis P., Deleflie F., Barlier F., *et al.* (2005) Effects of thermosphere total density perturbations on LEO orbits during severe geomagnetic conditions (Oct–Nov 2003) using DORIS and SLR data. Adv Space Res, vol 36(3), pp 522–533, DOI 10.1016/j.asr.2005.03.029

Willis P., Berthias J.-P., Bar-Sever Y. E. (2006) Systematic errors in the Z-geocenter derived using satellite tracking data, A case study from SPOT-4 DORIS data in 1998. J Geod, vol 79(10-11), pp 567–572, DOI 10.1007/s00190-005-0013-9

Willis P., Fagard H., Ferrage P., *et al.* (2010) The International DORIS Service (IDS) toward maturity. Adv Space Res, vol 45(12), pp 1408–1420, DOI 10.1016/j.asr.2009.11.018

Wu X., Abbondanza C., Altamimi Z., *et al.* (2015) KALREF-a Kalman filter and time series approach to the International Terrestrial Reference Frame realization. J Geophys Res Solid Earth, pp 3775–3802, DOI 10.1002/2014JB011622

Zelensky N. P., Lemoine F. G., Beckley D. B., Chinn D. S., Pavlis D. (2017) Impact of ITRS 2014 Realizations on Altimeter Satellite Precise Orbit Determination. Adv Space Res, DOI 10.1016/j.asr.2017.07.044